

# Image-Based Virtual Try-On: A Survey

Dan Song, Xuanpu Zhang, Juan Zhou, Weizhi Nie, Ruofeng Tong,  
Mohan Kankanhalli, *Fellow, IEEE*, and An-An Liu, *Senior Member, IEEE*

**Abstract**—Image-based virtual try-on aims to synthesize a naturally dressed person image with a clothing image, which revolutionizes online shopping and inspires related topics within image generation, showing both research significance and commercial potential. However, there is a big gap between current research progress and commercial applications and an absence of comprehensive overview of this field to accelerate the development. In this survey, we provide a comprehensive analysis of the state-of-the-art techniques and methodologies in aspects of pipeline architecture, person representation and key modules such as try-on indication, clothing warping and try-on stage. We propose a new semantic criteria with CLIP, and evaluate representative methods with uniformly implemented evaluation metrics on the same dataset. In addition to quantitative and qualitative evaluation of current open-source methods, we also utilize ControlNet to fine-tune a recent large image generation model (PBE) to show future potential of large-scale models on image-based virtual try-on task. Finally, unresolved issues are highlighted and future research directions are prospected to identify key trends and inspire further exploration. The uniformly implemented evaluation metrics, dataset and collected methods will be made public available at <https://github.com/little-misfit/Survey-Of-Virtual-Try-On>.

**Index Terms**—Virtual try-on, image synthesis, image warping, person representation, survey, AIGC.

## 1 INTRODUCTION

IMAGE-BASED virtual Try-On is a popular research topic in the field of AI-generated content (AIGC), specifically in the domain of conditional person image generation. It enables editing, replacement, and design of clothing image content, making it highly applicable in various domains such as e-commerce platforms and short video platforms [1]. In particular, online shoppers can benefit from virtual try-on by obtaining try-on effect images of clothing, thereby enhancing their shopping experience and increasing the likelihood of successful transactions. In addition, AI Fashion has also emerged on short video platforms, where users can edit the clothes worn by characters in images or videos according to their own creativity. This allows users to explore their sense of fashion and produce a wide range of engaging images and videos.

The concept of virtual try-on was proposed as early as 2001 [2], which uses a pre-calculated generic database to produce personally sized bodies and animate garments on a web application. Virtual try-on methods can be divided into three categories: physical-based simulation, real acquisition and image generation. Based on the cloth simulation techniques [3]–[5] as the core part, physical-based try-on simulation also involves human body reconstruction [6]–[15] and cloth measurement [16]–[18]. This kind of methods have the advantage in pose controllable and 360° display, but face

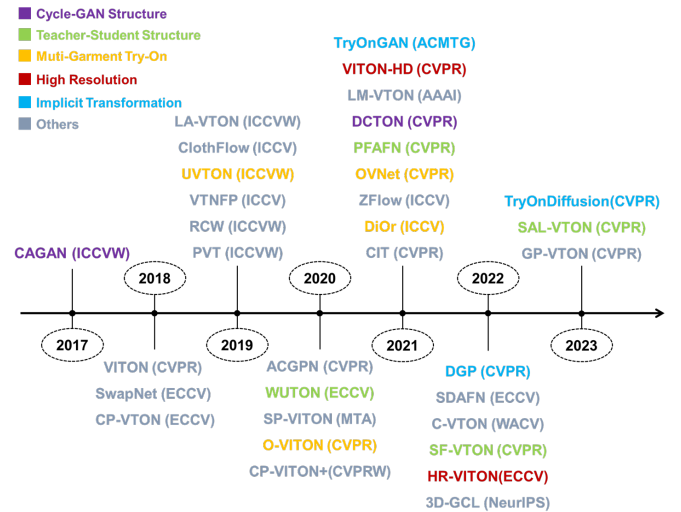


Fig. 1. A concise timeline of image-based virtual try-on milestones. Different colors indicate the main characteristic of method. Please refer to Table 1 for detailed comparisons.

plenty of difficulties in accuracy, efficiency and automation. Some brands, e.g., UNIQLO and GAP, employ this way as a virtual try-on solution. Real acquisition method usually captures and stores the appearance of apparel on a shape controllable robot for later displays, which shows high fidelity. Only a few companies, such as Fits.me, have adopted this approach, which requires massive labor for real acquisition. With the development of image generation techniques, image-based virtual try-on becomes appealing with benefits in high efficiency and low cost. However, the artifacts in generated images hinder its application to practical scenarios. Specifically, this paper focuses on image-based virtual try-on methods with a thorough review in

- D. Song, X. Zhang, J. Zhou, W. Nie and A.-A. Liu are the School of Electrical and Information Engineering, Tianjin University, Tianjin 300072, China.  
E-mail: dan.song@tju.edu.cn, anan0422@gmail.com
- R. Tong is with the College of Computer Science and Technology, Zhejiang University, Zhejiang 310058, China.
- M. Kankanhalli is with the School of Computing, National University of Singapore, Singapore.

This work was supported in part by the National Natural Science Foundation of China under Grant U21B2024 and Grant 61902277.  
Corresponding author: An-An Liu.

terms of methodology design and experimental evaluation, and further reveals unresolved issues leading to prospective future research directions.

Image-based virtual try-on can be regarded as one kind of conditional person image generation, which have undergone rapid development since 2017 (Fig. 1). Given a clothed person image and an in-shop clothing image, image-based virtual try-on aims to synthesize a naturally dressed body image. For this task, three main difficulties need to be overcome: 1) Obtaining high-quality supervised training data: It is almost impossible to acquire pairs of photographs where the same person is trying on two different garments in the same pose. 2) Achieving natural and realistic bending and shading of clothing in appropriate areas of the person body: It is challenging to ensure that the clothing adapts seamlessly and naturally to the contours of the body and appears realistic in terms of lighting and shadows. 3) Generating realistic try-on images: It is necessary to maintain consistency in non-clothing areas such as removing the original clothing residual uncovered by the new clothing and keep the person identity clear.

To overcome the above difficulties, tremendous efforts have been made and Fig. 1 show some representative methods on a timeline. In 2017, CAGAN [19] gave the first try by employing CycleGAN [20] to overcome the lack of training triplet data, i.e., (original person image, in-shop clothing image, try-on image), but the generation quality is far from satisfactory. Subsequently, VITON [21] creatively proposed clothing-agnostic person representation by human parsing to make up the lack of supervised training data. They constructed the basic network framework of “Try-On Indication + Cloth Warping + Try-on”, laying the foundation for further improvement on generation quality in subsequent works [22]–[31]. Apart from continuous quality improvements, some new goals are desired. Trying on multiple garments attracted attention in 2019 [32], but such works are scarce due to the complex interaction between multiple garments and the lack of specialized datasets [33]–[35]. In order to remove the heavy reliance on human parsing, several teacher-student networks were designed [36]–[38] to achieve parser-free try-on at inference time. Recently, with the advancement of computational capabilities, high-resolution virtual try-on tasks has become possible, e.g., VITON-HD [39] and HR-VTON [31]. Inspired by StyleGAN [40]–[43] and Diffusion model [44]–[47] in the field of image generation, single-stage networks [48], [49] as well as Diffusion architecture [50] emerged for this task.

In spite of the rapidly emerging works, there lacks a systematic survey to summarize image-based virtual try-on methods in datasets, method design and experimental evaluation. Two previous reviews [51], [52] only introduced several representative methods, but did not perform comprehensive comparison and unified evaluation. To the best of our knowledge, this is the first systematic image-based virtual try-on review with unified evaluation, which also has the following unique characteristics:

- **In-depth analysis.** We comprehensively review existing image-based virtual try-on methods from the perspectives of pipeline structures, human representations, clothing warping strategies, architectures of

try-on indication and image synthesis and corresponding loss functions.

- **Evaluation: unified evaluation, new criterion and user study.** We evaluate open-source works with the same dataset, and also perform user study on visual results with 333 volunteers. Particularly, we compute Semantic Score with CLIP [53] as a new criterion which can respectively evaluate the semantic similarity of try-on and non-try-on parts. Relevant data and codes will be publicly available at <https://github.com/little-misfit/Survey-Of-Virtual-Try-On>.
- **Open challenges and future directions.** According to the experimental results, we reveal a number of unresolved issues and draw important future research directions. Additionally, we utilize ControlNet [54] to fine-tune a recent large model (PBE [55]) for image-based virtual try-on, which shows the potentials and issues of popular large models on this task. We hope this review could spur the development of novel ideas towards image-based virtual try-on and its applications in industry.

The rest of this survey is organized as follows. Sec. 2 firstly gives the problem definition, and then comprehensively review the literature from multiple perspectives. Sec. 3 introduces datasets and evaluation criterion. Experimental results and analyses are presented in Sec. 4. Finally, we reveal unresolved issues Sec. 5 and prospect future directions in Sec. 6.

## 2 TECHNICAL REVIEW AND DISCUSSION

### 2.1 Overview

Image-based virtual try-on can be regarded as a conditional image generation task that uses in-shop clothing image  $I_c$  and person image  $I_p$  as raw data, and pre-processes the raw data as conditioned information to guide the model for generating try-on images  $I_{try-on} = G(I_p, I_c)$ . Three key modules are usually involved in image-based virtual try-on:

- **Try-On Indication** aims to provide a prior for guiding the deformation of clothing in the Cloth Warping module and the fusion of clothing and body in the Try-On module. It usually takes a combination of person body representations (e.g., semantic information [56], [57], Densepose [58], Openpose [59], [60] and so on) as input, and predicts the spatial structure of person body under the try-on state.
- **Cloth Warping** transforms the clothing image to the spatial distribution under the try-on state. The inputs of this module are clothing images and person body features such as cloth-agnostic person representation or dressed person representation obtained in the module of Try-On Indication. Via warping methods such as TPS [61], STN [62], and FlowNet [63] that transform the spatial positions of pixels/feature points, the output this module could be warped clothing images or deformed clothing features.
- **Try-On module** generates the final try-on image by fusing the person body and clothing features. Interpolation or generative networks are designed

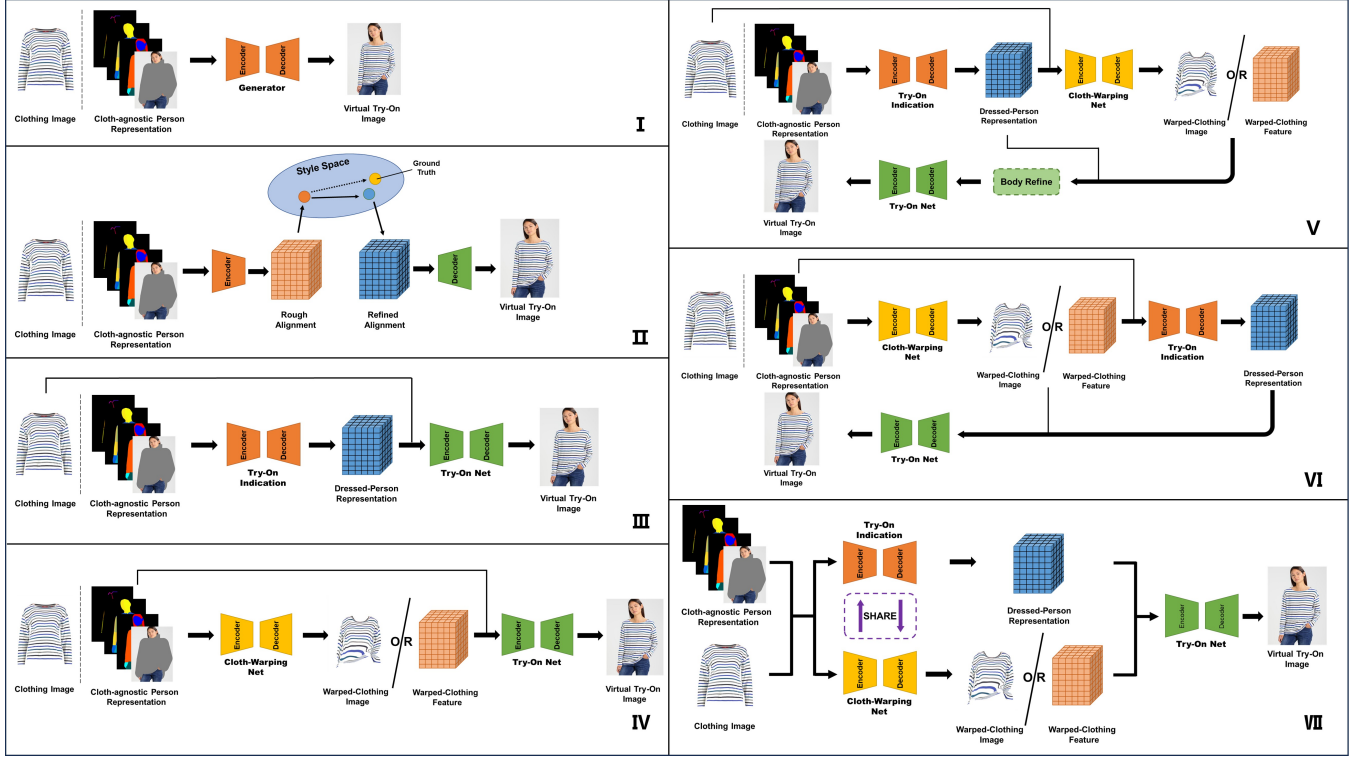


Fig. 2. Basic pipelines of image-based virtual try-on. Pipelines I and II are both single-stage approaches, where pipeline I utilizes a single generator to directly generate the try-on image, while pipeline II aligns features in the feature domain before generating the try-on image. Pipelines III and IV are both two-stage pipelines, where the former utilizes person representation as the bridge while the later uses warped clothing. Pipelines V and VI are three-stage pipelines, which differ in the order of Try-On Indication and Cloth Warping. Pipeline VII is an improvement over V and VI, which simultaneously performs Try-On Indication and Cloth Warping, with/without both modules communicating during the data processing. For detailed explanations of the Try-On Indication, Cloth Warping, and Try-On module, please refer to Section 2.4, 2.5, 2.6.

for this module, and the output image should meet the following requirements: 1) the clothing within the try-on area should be clear and natural, 2) the content outside the try-on area (excluding the original clothing that is planned to take off) should remain unchanged, and 3) there should be a correct semantic relationship between the new clothing and the person body.

It is worth noting that the above three steps are not necessarily present at the same time, and there is no strict order. Table 1 summarizes representative methods and we will discuss the key designs in the following subsections.

## 2.2 Pipelines

In the virtual try-on pipeline, the selection and placement of the aforementioned three modules have a significant impact on the final try-on results. As shown in Fig. 2, the basic pipeline structure can be categorized into seven types. Type I and II are one-stage pipelines and the later one additionally introduces feature alignment. Type III and IV are two-stage pipelines which respectively utilize person representation and warped clothing as intermediate generation for further optimization. The rest types are three-stage pipelines, where type V and VI differ in the order of Try-On Indication and Cloth Warping modules while type VII simultaneously optimizes these two modules. The pipeline choice of representative methods can be found in Table 1, with no obvious preference in the development trend.

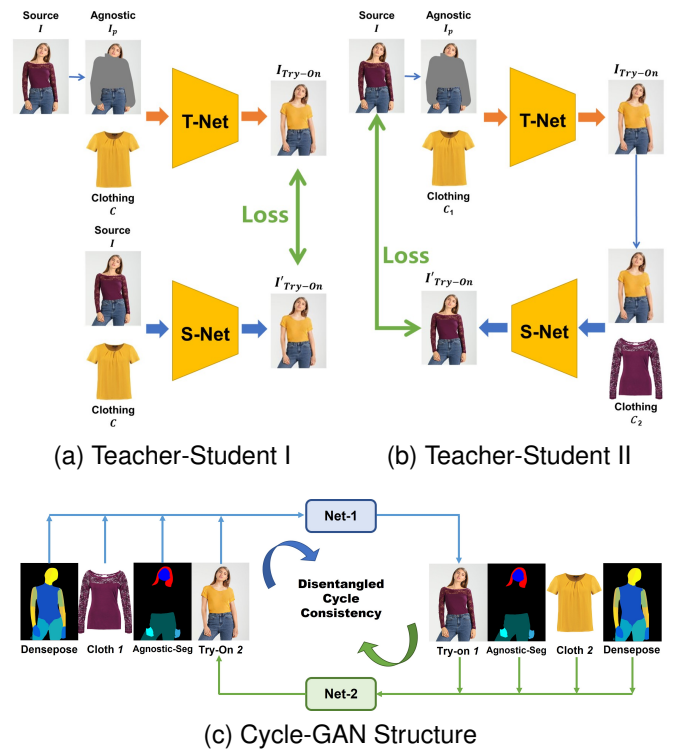


Fig. 3. Three supplemental structures: (a) Teacher-Student network involving one set of in-shop clothes; (b) Teacher-Student network involving two sets of clothes; (c) Cycle-GAN structure with two sets of clothes.

TABLE 1

Key characteristics of representative image-based virtual try-On methods. Please refer the number of pipeline to Fig. 2 and the number of person representation is shown in Fig. 4. The three loss items are the respective losses for modules of Try-On Indication, Cloth Warping and Try-on. “-” means this item is not available or not indicated in the published work.

|      | Model                | Source         | Pipeline  | Person Rep. | Try-On Indication     | Loss   | Cloth Warping         | Loss  | Try-On                          | Loss   | Train/Test Set           |
|------|----------------------|----------------|---|-------------|-----------------------|--|-----------------------|---|---------------------------------|--|--------------------------|
| 2017 | CAGAN [19]           | ICCVW          | I   | 1           | -                     | -  | -                     | -   | Cycle-GAN Mask Combine          | Mask L1<br>Cycle Loss<br>Adversarial Loss  | Zalando SE               |
| 2018 | SwapNet [64]         | ECCV           | II  | 2,10        | DualPath U-Net        | Adversarial Loss<br>Cross Entropy Loss         | -                     | -   | U-Net                           | Mask L1<br>Perceptual Loss<br>Adversarial Loss   | DeepFashion / VITON      |
|      | VITON [21]           | CVPR           | V   | 2,5,6       | U-Net                 | Mask L1<br>Perceptual Loss                     | TPS                   | -   | Mask Combine                    | Mask L1<br>Perceptual Loss<br>Mask TV Norm   | VITON                    |
|      | CP-VTON [23]         | ECCV           | VI  | 2,5,6       | U-Net                 | -  | TPS                   | L1 Loss   | Mask Combine                    | Mask L1<br>L1 Loss<br>Perceptual Loss  | VITON                    |
| 2019 | RCW [27]<br>PVT [28] | ICCVW<br>ICCVW | Use PatchGAN method to train GMM module in CP-VTON<br>Add semantic information assisted training GMM in CP-VTON |             |                       |  |                       |   |                                 |  |                          |
|      | LA-VTON [29]         | CVPR           | VI  | 2,5,7       | U-Net                 | Mask L2  | TPS                   | L1 Loss<br>Adversarial Loss<br>Grid Interval Consistency  | Mask Combine<br>Refine Net      | L1 Loss<br>Perceptual Loss<br>Adversarial Loss   | VITON                    |
|      | UVTON [32]           | ICCVW          | III   | 2,9         | Multi-GAN             | L1 Loss<br>Perceptual Loss<br>Adversarial Loss | -                     | -   | U-Net                           | L1 Loss<br>Perceptual Loss<br>Adversarial Loss   | VITON                    |
|      | VTNFP [30]           | ICCV           | VI  | 2,4,5,11    | CNN                   | Adversarial Loss<br>Focal Loss [65]            | TPS                   | L1 Loss<br>Adversarial Loss                               | Attention U-Net<br>Mask Combine | Mask L1<br>L1 Loss<br>Perceptual Loss  | VITON                    |
|      | Clothflow [66]       | ICCV           | V   | 1,5,10      | U-Net                 | Cross Entropy Loss                             | FlowNet               | ROI Perceptual Loss<br>Mask L1<br>TV Norm                 | U-Net                           | Perceptual Loss<br>Style Loss  | DeepFashion / VITON      |
| 2020 | SP-VITON [25]        | MTA            | V   | 2,5,8       | U-Net                 | Mask L1<br>Perceptual Loss                     | TPS                   | -   | U-Net<br>Mask Combine           | Perceptual Loss<br>Mask L1<br>Mask TV Norm   | VITON                    |
|      | CP-VTON+ [22]        | CVPRW          | VI  | 2,5,7       | U-Net                 | Mask L1  | TPS                   | Mask L1<br>Grid Regularization                            | U-Net<br>Mask Combine           | Mask L1<br>L1 Loss<br>Perceptual Loss  | VITON                    |
|      | WUTON [36]           | ECCV           | IV  | 3           | -                     | -  | TPS                   | L1 Loss   | Siamese U-Net                   | Adversarial<br>L1 Loss<br>Perceptual Loss  | VITON                    |
|      | ACGPN [26]           | CVPR           | V   | 2,4,11      | Multi-GAN             | Adversarial Loss<br>Cross Entropy Loss         | TPS                   | L1 Loss<br>Second-order-difference<br>Constraint [67]     | Body Part-<br>Composition GAN   | Adversarial Loss   | VITON                    |
|      | O-VITON [33]         | CVPR           | V   | 9,10        | Auto-Encoder          | Adversarial Loss<br>Cross Entropy Loss         | -                     | -   | Broadcast Decoder               | Mask L1<br>L1 Loss<br>Perceptual Loss  | VITON                    |
| 2021 | LM-VTON [24]         | AAAI           | VI  | 2,5,11      | U-Net                 | Adversarial Loss<br>Cross Entropy Loss         | TPS                   | L1 Loss<br>LandMark Loss<br>Perceptual Loss<br>Mask L1    | U-Net                           | L1 Loss<br>Adversarial Loss<br>Perceptual Loss   | VITON<br>MPV             |
|      | OVNet [34]           | CVPR           | V   | 5,12        | U-Net                 | Cross Entropy Loss<br>LSGAN Loss [68]          | Multi-STN             | Cascade Loss  | U-Net                           | L1 Loss<br>Hinge-<br>Adversarial Loss [69]<br>Perceptual Loss  | Self Made<br>/ VITON     |
|      | CIT [70]             | CVPR           | VI  | 4,5,7       | Transformer-<br>U-Net | Mask L1  | Transformer-<br>TPS   | L1 Loss<br>Grid Regularization                            | U-Net<br>Mask Combine           | L1 Loss<br>Perceptual Loss   | VITON                    |
|      | DCTON [71]           | CVPR           | IV  | 1,8         | -                     | -  | TPS                   | L1 Loss<br>Homography Matrix Reg                          | CNN                             | L1 Loss<br>Adversarial Loss<br>Content Preserving Loss<br>Perceptual Loss  | VITON<br>VITON-HD        |
|      | PFAFN [37]           | CVPR           | IV  | 5,8,12      | -                     | -  | FlowNet               | Second-order-<br>smooth Constraint                        | U-Net                           | L1 Loss<br>Perceptual Loss   | MPV<br>VITON<br>VITON-HD |
|      | VITON-HD [39]        | CVPR           | V   | 3,5,12      | U-Net                 | Adversarial Loss<br>Cross Entropy Loss         | TPS                   | Second-order-difference<br>Constraint [67]                | ALIAS Generator                 | Adversarial Loss<br>Feature Matching loss<br>Perceptual Loss   | VITON                    |
|      | DiOr [35]            | ICCV           | IV  | 1,5         | -                     | -  | FlowNet               | -   | Broadcast Decoder               | L1 Loss<br>Perceptual Loss<br>Style Loss<br>Adversarial Loss<br>Cross Entropy Loss<br>Geometric Loss                   | DeepFashion              |
|      | ZFlow [72]           | ICCV           | VII   | 4,5,7,8,9   | U-Net                 | Cross Entropy Loss                             | FlowNet               | L1 Loss<br>Perceptual Loss<br>Mask L1<br>TV Norm          | U-Net<br>Mask Combine           | L1 Loss<br>Perceptual Loss<br>Edge Loss<br>Segment-<br>Cross Entropy Loss<br>Densepose-<br>Cross Entropy Loss<br>UV L1 | VITON                    |
|      | TryOnGAN [48]        | ACMTG          | II  | 1           | -                     | -  | Implicit<br>Transform | -   | StyleGAN2                       | Editing-localization Loss<br>Identity Loss<br>Projection Loss<br>Garment Perceptual Loss                               | Self-Made                |
| 2022 | Flow-Style-VTON [38] | CVPR           | IV  | 5,8,12      | -                     | -  | FlowNet               | -   | U-Net                           | L1 Loss<br>Garment L1 Loss<br>Flow-smooth Reg<br>Distillation Loss   | VITON                    |
|      | DGP [49]             | CVPR           | II  | 13          | -                     | -  | Implicit<br>Transform | -   | Decoder                         | L2 Loss<br>Perceptual Loss<br>Adversarial Loss<br>Attribute Loss   | ESF<br>/ CMI MPV         |
|      | HR-VITON [31]        | ECCV           | VII   | 3,8,12      | Dualpath-<br>U-Net    | Cross Entropy Loss                             | FlowNet               | Mask L1<br>Adversarial Loss<br>Perceptual Loss<br>TV Norm | Mask Combine<br>Decoder         | Adversarial Loss<br>Perceptual Loss<br>Feature Matching loss   | VITON-HD                 |
|      | C-VTON [73]          | WACV           | IV  | 3,8         | -                     | -  | TPS                   | Mask L1<br>L1 Loss<br>Perceptual Loss                     | U-Net                           | Perceptual Loss<br>DensePose-<br>Adversarial Loss<br>Garment-<br>Adversarial Loss<br>Body-<br>Adversarial Loss         | MPV<br>VITON             |
|      | SDAFN [74]           | ECCV           | IV  | 3,4         | -                     | -  | Multi-<br>FlowNet     | -   | Decoder                         | Multi Layer:<br>L1 Loss<br>Style Loss<br>Perceptual Loss   | MPV<br>VITON             |



|      | Model                | source  | Pipeline | Person Rep. | Try-On Indication | Loss                                   | Cloth Warping | Loss  | Try-On                 | Loss   | Train/Test Set         |
|------|----------------------|---------|----------|-------------|-------------------|--|---------------|---|------------------------|--|------------------------|
| 2022 | 3D-GCL [75]          | NeurIPS | IV       | 9           | -                 | -                                      | FlowNet       | L1 Loss<br>Perceptual Loss<br>3D Regularization                             | StyleGAN2              | L1 Loss<br>Perceptual Loss<br>Adversarial Loss               | MPV<br>DeepFashion     |
| 2023 | GP-VTON [76]         | CVPR    | VII      | 5,8,12      | Dualpath-U-Net    | Cross Entropy Loss<br>Adversarial Loss | Multi-FlowNet | L1 Loss<br>Mask L1<br>Perceptual Loss<br>Second-order<br>-smooth Constraint | Mask Combine<br>+U-Net | L1 Loss<br>Mask L1<br>Adversarial Loss<br>Perceptual Loss    | VITON-HD<br>Dress Code |
|      | SAL-VTON [77]        | CVPR    | VII      | 1,13        | -                 | -                                      | Multi-FlowNet | L1 Loss<br>LandMark Loss<br>Perceptual Loss<br>Smoothness Norm [78]         | U-Net                  | Adversarial Loss<br>Perceptual Loss<br>Feature Matching loss | VITON<br>VITON-HD      |
|      | TryOn Diffusion [50] | CVPR    | I        | 4           | -                 | -                                      | -             | -   | Large Model            | Diffusion Denosing Loss                                      | MPV<br>VITON           |

Supplemental to the basic try-on image generation pipeline, Fig. 3 shows other structures such as Teacher-Student network [36]–[38] and Cycle-GAN [20], [77]. The Teacher-Student architecture is mainly designed for training parser-free try-on network and Fig. 3a shows the straightforward implementation [36]. PFAFN and Style-Flow-VTON [37], [38] further improve it to Fig. 3b where the synthesized image generated by the teacher network  $I_{try-on}$  is used as the input of the student network. Compared with type 1, type 2 provides more reliable supervision with the ground truth in case that the teacher network generates poor results. Similarly, the adoption of Cycle-GAN [20], [77] (Fig. 3c) also shows a strategy for using cycle consistency to enhance the supervision in try-on.

### 2.3 Cloth-agnostic Person Representation

In practical scenarios, it is difficult to acquire the triplet (person image  $I_s$ , in-shop clothing image  $C_t$ , try-on image  $I_t$ ) for training. Instead, pairs of person image and in-shop clothing image are commonly seen. Therefore, cloth-agnostic person representation is studied to remove the clothing that is planned to take off, and constitute the triplet (cloth-agnostic person representation  $I_{agnostic}$ , in-shop clothing image  $C_t$ , person image  $I_t$ ) for supervised training. Existing works employ human parser to extract representations such as pose, shape and semantic distribution from the person body. As shown in Fig. 4, the representations can be categorized into different types: RGB image  $\mathcal{P}_{1,2,3,4}$ , pose keypoints  $\mathcal{P}_5$ , silhouette  $\mathcal{P}_{6,7}$ , Densepose  $\mathcal{P}_{8,9}$ , semantic segmentation  $\mathcal{P}_{10,11,12}$ , and landmark  $\mathcal{P}_{13}$ .

RGB image  $\mathcal{P}_{1,2,3,4}$  provides pixel-level features that can better preserve the identity information of individuals and the content outside the try-on area.  $\mathcal{P}_1$  shows the original person image which is disturbed by the original clothes.  $\mathcal{P}_{2,3,4}$  can be acquired via human parsing [56], [60], where  $\mathcal{P}_2$  contains the head information,  $\mathcal{P}_3$  masks the try-on related area using large areas of gray pixels, and  $\mathcal{P}_4$  deletes the masked area with background color. Comparatively,  $\mathcal{P}_3$  contains some clues about pose and shape while  $\mathcal{P}_4$  completely removes the try-on related body area.

Pose features  $\mathcal{P}_5$  [59], [60] estimate the positions of 18 key points of the body, which provides an important condition for generating person body images and directly affects clothing deformation.

Silhouette  $\mathcal{P}_{6,7}$  refers to the body contour that contains rough pose and shape information. Cloth-agnostic representation was initially proposed by VITON [21] via down-sampling to a lower resolution to make the contour unclear about the original clothes.

To further separate the shape representation from original clothes, SP-VITON [25] initially utilizes Densepose [58] to estimate the body shape under clothes. Densepose also provides other formats such as semantic parsing  $\mathcal{P}_8$  and UV map coordinates  $\mathcal{P}_9$  corresponding to the 3D model.

Semantic segmentation  $\mathcal{P}_{10,11,12}$  is used to provide knowledge about the try-on area in virtual try-on. However, the contour of semantic distribution  $\mathcal{P}_{10}$  indicates the original clothes and has negative impacts on trying on new clothes. Consequently, a combination of clothes and related skin  $\mathcal{P}_{11}$  aims to eliminate the prior influence of the original clothing style. Furthermore,  $\mathcal{P}_{12}$  completely removes the contour of the original clothing, retaining only the semantic regions unrelated to the try-on area. Although totally getting rid of the original clothes, the complete deletion also loses body shape priors.

Landmark  $\mathcal{P}_{13}$  provides explicit semantic information for shape alignment. It guides clothing deformation by constraining the distance between clothing landmarks and corresponding body landmarks. SAL-VTON [77] makes improvements based on HR-Net [79] and proposes a Landmark estimation network. To train this network, an open source landmark dataset has been annotated on three mainstream datasets: VITON [21], VITON-HD [39], and Dress-Code [80]. The landmark shown in the Fig. 4 are derived from [49] but have not been made publicly available yet.

The choices of representative methods are shown in Table 1, where pose keypoints are most commonly used and silhouette falls behind the other types. Additionally, there is no obvious preference towards representation types and a combination of several types could also be used.

### 2.4 Try-On Indication

Given the cloth-agnostic person representation and target clothing information as input, the Try-On Indication network (i.e., the orange module in Fig. 2) is used to predict the dressed person representation, which directly influences the generation of the final try-on image. The architectures of this module and corresponding constraint losses for representative methods are shown in Table 1, where the encoder-decoder structure is the mainstream framework for Try-On Indication. It encodes cloth-agnostic person representation and decodes the representation of dressed person under the condition of the target clothing.

VITON-series works [21]–[23], [25], [27]–[30] such as VITON [21] and CP-VTON [23] use the U-Net [81] architecture and person representation  $\mathcal{P}_{2,5,6}$  to directly generate coarse try-on images, but sometimes generate blurry trunk and misalignment of the clothing edges. To overcome this issue,

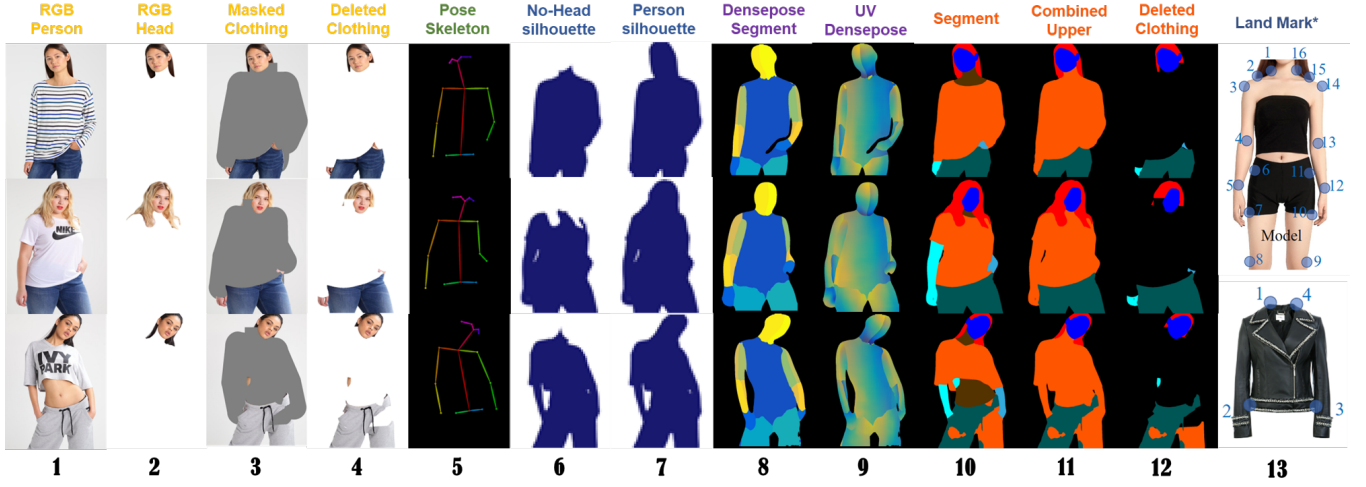


Fig. 4. Person representation types. Existing representations heavily rely on human parsers to indicate pose, shape or semantic segmentation, which can be categorized into different types: RGB image  $\mathcal{P}_{1,2,3,4}$ , pose  $\mathcal{P}_5$ , silhouette  $\mathcal{P}_{6,7}$ , Densepose  $\mathcal{P}_{8,9}$ , semantic segmentation  $\mathcal{P}_{10,11,12}$ , and landmark  $\mathcal{P}_{13}$ . \* Subfigures of  $\mathcal{P}_{13}$  are cited from [49].

CIT [70] added the Transformer [82] structure to the basis of CP-VTON, but still cannot totally solve this problem.

Instead of predicting pixels of rough try-on images, ClothFlow [66] uses U-Net to estimate the semantic distribution of dressed persons. Some other works [24], [26], [34], [39], [72] such as ACGPN [26] and LM-VTON [24] follow the same strategy and combine the person representation with  $\mathcal{P}_{2,5,6,7,8,11}$ , further improving the try-on effects.

Instead of single-step prediction, multiple steps could also improve the generation quality. UVTON first takes  $\mathcal{P}_4$  and clothing images as input, generates RGB images of ten body areas through ten generators, and then uses this set of images and  $\mathcal{P}_{4,9}$  to generate coarse try-on images. ACGPN [26] proposes a Try-On Indication composed of two serial GAN generators. The first generator uses  $\mathcal{P}_{5,11}$  features and clothing images to predict the semantic distribution. Then the predicted semantic distribution, pose keypoints  $\mathcal{P}_5$  and clothing images are input into the second generator to predict the mask of the clothing area. O-VITON [33] introduces a shape generation network, which first encodes the shapes of different body parts, and then inputs the encoding values and UV Densepose  $\mathcal{P}_9$  into the generator to generate the semantic map.

Indeed, the Try-On Indication module and the Clothing Warping module are closely related and affect each other. HR-VTON [31] inputs clothing images, clothing Masks and person representation  $\mathcal{P}_{8,13}$  at the same time, and simultaneously generates warped clothes and person’s semantic distribution. The warping path and the semantic prediction path can keep communication through the Fusion Block.

As shown in Table 1, the commonly-used loss for constraining Try-On Indication module mainly involve mask L1/L2, cross entropy loss, adversarial loss and perceptual loss. Specifically, mask L1/L2 is used to constrain the clothing mask, cross entropy loss facilitates the segmentation prediction and perceptual loss is designed for the generated RGB image. Adversarial loss is adopted for GAN-based generation methods. Both of Focal loss [65] and LSGAN loss [68] are designed to constrain the generation of segmentation.

## 2.5 Cloth Warping

Shown as the yellow module in the pipeline (Fig. 2, Cloth Warping module aims to transform the spatial distribution of the clothing image/feature to match the body. The mainstream deformation methods can be classified into: Thin Plate Spline (TPS), Spatial Transformation Network (STN), Flow Net and Implicit transformation. The choices of representative methods and corresponding losses are illustrated in Table 1.

### 2.5.1 Thin Plate Spline

Thin Plate Spline (TPS) interpolation method use the deformation of a thin steel plate to simulate 2D deformation, which is utilized for warping clothes in the literature [21]–[25], [27]–[29], [39], [70], [73]. Suppose there are  $N$  control points (e.g., the nodes of image grid shown in Fig. 5a), we denote the original coordinates as  $T = (t_1, t_2, \dots, t_n)^T$  and target coordinates as  $Y = (y_1, y_2, \dots, y_n)^T$ . Take one point  $y_i$  as an example, its interpolation under TPS transformation can be formulated as:

$$\Phi(y_i) = c + \mathbf{A}\mathbf{y}_i + \sum_j^N (w_j U(\|\mathbf{y}_i - \mathbf{t}_j\|)) \quad (1)$$

where  $c$  and  $A$  simulate linear transformation,  $U(\cdot)$  represents a collection of radial basis functions, and  $w_i$  is the corresponding weighting parameter. Please refer to [61] for more details.

Given a series of control points and their target positions, target image under TPS interpolation could be computed. However, for image-based virtual try-on, the lack of ground truth for target positions becomes an obstacle for TPS-based methods. VITON utilize shape context matching [130] to estimate target positions based on the context relationship of the clothing mask and the predicted warped mask. WUTON [36] uses TPS transformation at the feature level, which can enhance the diversity of clothing warping but has a shortage of image clarity. CP-VTON [23] designs a Geometry Matching Module (GMM, one type of Spatial Transformer

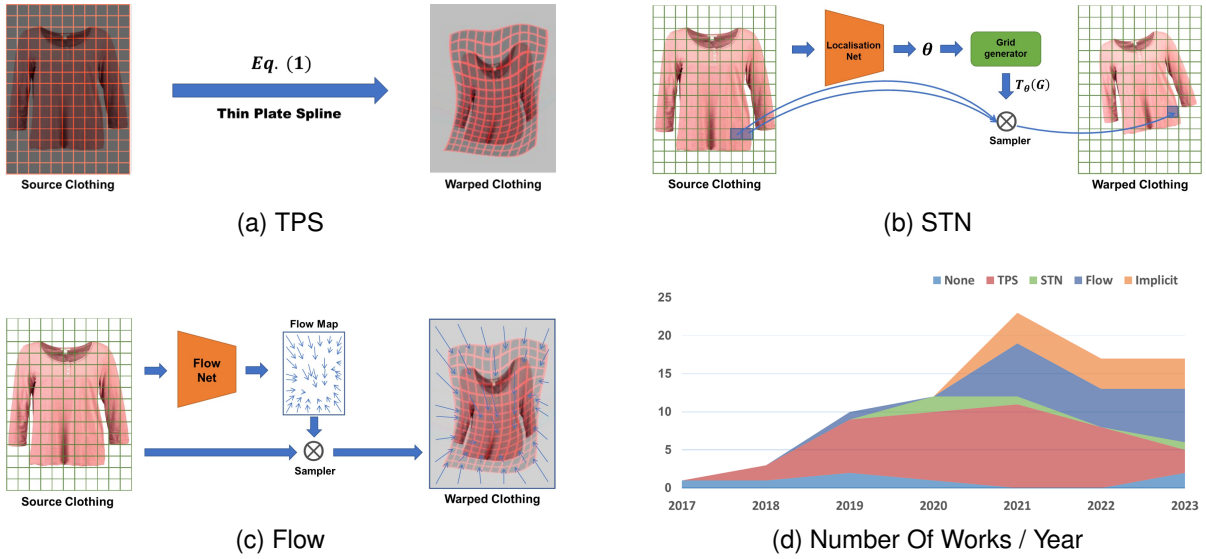


Fig. 5. Illustration for several spatial transformation approaches: (a) Thin Plate Spline (TPS), (b) Spatial Transformation Network (STN) and (c) Flow. (d) shows the usage statistics of various methods obtained after analyzing the literature listed in Table 1 and [83]–[129].

Network) to feed  $\mathcal{P}_{2,5,6}$  and learns TPS parameters for clothing warping. CP-VTON uses pixel-level L1 loss of warped clothing image to train GMM.

With the help of spatial transformation network (STN, which will be introduced next), further trials have been made to better constrain TPS transformation: 1) Regularization. To constrain the warping of clothing, CP-VTON+ [22] introduces a regularization term that calculates the sum of distance changes for  $N$  nodes of grid; LA-VTON [29] proposes the constraint of grid interval consistency, which limits the distance between adjacent nodes; ACGPN [26] proposes a second-order difference constraint to prevent exaggerated deformation; DCTON [71] uses a homography matrix  $H$  to reduce the change of the transformation matrix. 2) Auxiliary information. LM-VTON [24] designs a landmark-based method for fine-grained constraint. VITON-HD [39] additionally uses  $\mathcal{P}_{3,5}$  and the clothing region Mask, while C-VTON [73] uses Densepose features alone as the input of GMM. 3) New model. CIT [70] replaces the association layer in GMM with Transformer structure to better calculate the spatial correlation between the person pose and the clothing.

### 2.5.2 Spatial Transformation Network

Spatial Transformation Network (STN) [62] can be embedded into a layer of the network, and consists of three main parts as shown in Fig. 5b: 1) Localisation Network is a simple regression network which contains several convolutional layers to regress  $N$  variables (for example, a  $2 \times 3$  matrix with 6 variables in the case of affine transformation). 2) Grid Generator is responsible for calculating the coordinates of the target image corresponding to the coordinates of the original image through matrix operations with  $T_\theta(G)$ . 3) Sampler samples the original image according to the coordinates in  $T_\theta(G)$  and copies the pixels from original image to target image.

To simulate complex garment deformation, single STN usually cooperates with TPS, such as GMM in CP-VTON

[23]. Multiple STNs are another way to capture complex deformations by iteratively performing multiple transformations (e.g., affine transformation). OVNet [34] decomposes the warping of clothing into multiple small warps with excellent results, which proposes a multi-warp clothing generator to obtain  $k$  warping results. The  $k$  deformed images are connected in the channel scale and input into the Try-On module together to facilitate the generation of try-on image.

### 2.5.3 Flow Estimation

Flow indicates the offset of pixel or feature before and after transformation. Let  $(u_x, u_y)$  denote the offset, the value at target position  $(x, y)$  can be sampled at  $(x - u_x, y - u_y)$  in the original distribution, and the non-integer coordinates are interpolated by bilinear interpolation. Flow estimation methods for cloth warping can be classified in terms of prediction target such as pixel and feature or prediction steps such as single layer or multiple layers.

Dior [35] employs a single-layer flownet to deform the clothing features, where GFFE (Global Flow Field Estimator) proposed by GFLA [131] is used to predict flow map and soft mask. To capture more 3D changes of human posture deformation, 3D-GCL [75] uses [63] to create SMPL [132] flows as ground truth to constrain flow map, which results in better visual outcomes on the Deep Fashion data set.

A single-layer flownet applies sampling just at one level, while a multi-layer flownet conducts sampling from coarse to fine across multiple feature levels. ClothFlow [66] adopts a dual-path multi-layer decoder, which performs flow map calculation and warping at the feature level in each layer. Finally, the pixel-level flow map is output in the last layer. Similar to the structure of flownet in Clothflow, PFAFN [37] uses more human parsing features  $\mathcal{P}_{5,8,13}$  to guide the estimation of Flownet. To extract more flow features, ZFlow [72] procures flow maps of identical sizes from various depths within U-net via interpolation, which are then consolidated into a single flow map. Intuitively, this is a pixel-by-pixel

selection process, which determines the total flow rate by selecting (allowing or excluding) the pixel flow estimation of different radial neighborhoods (for multiple scales). In order to prevent excessive deformation caused by the high degree of freedom of flowNet, total variation loss is added to the loss function as a regularization term.

There are also some other interests in flow estimation. HR-VTON [31] and SDAFN [74] put emphasis on the coupling between body features and clothing. To counteract the potential image distortion resulting from FlowNet’s excessively focus on local alignment, Flow-Style-VTON [38] uses StyleGAN network to capture global deformation information to generate a coarse flow map, and then refines it locally to output target flow map. To achieve the refinement of flow estimation, multi-flow is gaining increasing popularity. SDAFN [74], SAL-VTON [77] and GP-VTON [76] construct a warping network from coarse to fine. Compared with the general flownet, they use multiple flow maps to estimate multiple factors such as posture, body shape and mask of clothing.

#### 2.5.4 Implicit Transformation

In O-VITON [33], TryOnGAN [48], and DGP [49], no explicit spatial transformation method is adopted, but after deep encoding, the clothes is aligned to the target posture in the feature space. O-VITON, as an early work adopting implicit transformation, simply diffuses clothing features in the corresponding person body region. TryOnGAN and DGP are recent works, which adopt the alignment in the feature space of StyleGAN [41], [42] to deform clothing to the target posture, achieving seamless coverage of the person body.

As shown in Fig. 5d, there has been a diversification in clothing warping methods in recent years. Single-STN methods are unable to handle natural deformation. Apart from a few works employing Multi-STN, most methods use a combination of STN and TPS, and they are classified under the TPS category. Influenced by the GMM framework, TPS transformation is the most popular method. TPS transformations have limitations in terms of degrees of freedom for deformation. In order to achieve more diverse clothing warping results, flow estimation has become a breakthrough in deformation performance. At the cost of greater computational overhead, flownet has achieved stronger deformation capabilities, and its usage is on the rise. Implicit transformation methods deform garments in a generative manner, further enhancing the diversity of garment deformation but also posing challenges in controlling clothing content. With the development of image generation technology under the diffusion framework, implicit transformation methods become promising.

Two kinds of loss for clothing warping are commonly adopted: 1) L1 loss and perceptual loss to supervise the warping with ground truth; 2) Regularization to alleviate exaggerated deformation, such as grid interval consistency, second-order-difference constraint, landmark loss, grid regularization, homography matrix regularization and TV (total variation) norm.

## 2.6 Try-On

Try-On module is the final stage of the try-on pipeline, which combines the clothing and person information obtained in the previous modules to generate the final try-on image. Therefore, it directly affects the quality of the output image. At present, there are two kinds of methods in the literature, one is to use mask for combining the person image and the warped clothing image [21]–[23], [25], [27], [28], [70], and the other is using the generation network with the clothing and person features [24], [26], [29], [31]–[39], [48], [49], [64], [66], [71], [72], [74]. Comparatively, the latter one obtains better generation performance at the cost of computation, which is the current mainstream approach.

**Mask Combination:** Some methods [19], [21]–[23], [25], [27], [28], [70] adopt the mask combination to generate the final try-on image, which is formulated as  $I = I_{coarse} \cdot (1 - M) + C \cdot M$ . The input is the coarse try-on image  $I_{coarse}$ , the warped clothing image  $C$  and the mask  $M$  representing the clothing region of the dressed person. Essentially, the warped clothing is covered in the area represented by the  $M$  in the  $I_{coarse}$ . This is a relatively simple and direct method, the advantage of which is that it will not increase the number of network parameters, but the disadvantage is that the quality of the final try-on image  $I$  depends entirely on the correctness of the clothing warping and the coarse try-on image where misaligned regions cause artifacts.

**Generation:** Generation-based methods [24], [26], [29], [31]–[39], [48], [49], [64], [66], [71], [72], [74], [75] all use a generator to design the Try-On module. Among them, [30], [34], [36]–[38], [64], [72] use U-Net as the generator. Besides the try-on image as the generation target, VTNFP [30] uses U-Net to generate the try-on image and the combination mask at the same time, where combination mask is used to optimize the clothing details of the try-on image. The U-Net in ZFlow [72] additionally generates representation features  $\mathcal{P}_{8,9,10}$  and calculates the loss between these three features and the ground truth to assist the training of the Try-On network.

For high-resolution virtual try-on [31], [39], misalignment regions between the clothing and the person body become more pronounced, and special designs for the generator are expected to eliminate the misalignment between clothing and body. VITON-HD [39] uses ALIAS ResBlock in the decoder part of the generator, and retains better spatial distribution information of clothing and person features through SPADE [133] normalization when generating try-on images. Moreover, it explicitly calculates the misalignment area between person and clothing in the residual block, guiding the network to fill the texture features of clothing into the misalignment area. In HR-VITON [31], the dressed person semantic distribution and the warped clothing image are aligned first, eliminating the misaligned areas. To constrain the complex process of semantic map processing, a “discriminator rejection method” was proposed to eliminate the low-quality semantic information map during adversarial training.

Previously, only using the Try-On module (without explicit try-on indication and cloth warping) could only generate rough try-on images. However, this issue has been alleviated in the era of large-scale models. TryOnDiffusion

TABLE 2

Key properties of datasets. Popularity refers to the number of usage that is summarized from the literature listed in Table 1 and [83]–[127].

| Data Set    | Year | Clothing Image | Women | Men | Upper body | Lower body | Full body | Multi Pose | Human Parsing | Resolution                            | Quantity Train/Test | Popularity |
|-------------|------|----------------|-------|-----|------------|------------|-----------|------------|---------------|---------------------------------------|---------------------|------------|
| VITON       | 2018 | ✓              | ✓     | ✗   | ✓          | ✗          | ✗         | ✗          | ✓             | $256 \times 192$<br>$1024 \times 768$ | 14,221/2,032        | 47         |
| MPV         | 2019 | ✓              | ✓     | ✗   | ✓          | ✗          | ✗         | ✓          | ✓             | $256 \times 192$                      | 52,236/10,544       | 11         |
| DeepFashion | 2016 | ✗              | ✓     | ✓   | ✓          | ✓          | ✓         | ✓          | ✓             | $1101 \times 750$                     | 52,712/-            | 11         |
| VITON-HD    | 2021 | ✓              | ✓     | ✗   | ✓          | ✗          | ✗         | ✗          | ✗             | $1024 \times 768$                     | 11,647/2,032        | 11         |
| ESF         | 2022 | ✗              | ✓     | ✓   | ✓          | ✗          | ✓         | ✗          | ✗             | $512 \times 512$                      | 170,000/10,000      | 1          |
| Dress Code  | 2022 | ✓              | ✓     | ✓   | ✓          | ✓          | ✓         | ✗          | ✓             | $1024 \times 768$                     | 48,392/5,400        | 8          |

[50] has designed a substantial Parallel-UNet, which, after being trained with massive amounts of data, can directly use the original image and pose features to accomplish high-quality try-on.

As illustrated in Table 1, besides the commonly-used L1 loss, perceptual loss and adversarial loss, some works further design local constraint (e.g., content preserving loss [71] and editing-localization loss [48]) and additional semantic constraint (e.g., feature matching loss [39] and attribute loss [49]).

### 3 DATASETS AND EVALUATION CRITERIA

#### 3.1 Datasets

In this section, we will introduce the currently public virtual try-on datasets. Before showing the details of each dataset, Table 2 compares them in terms of several key characteristics and counts the usage quantities of various datasets. VITON [21] is the first dataset for image-based virtual try-on and also the most popular one. Fig. 6 visually shows the samples for each dataset.

**VITON** dataset was released by Han et al. [21] in 2018, which collected a total of 16,253 pairs of top clothing images and frontal-view woman images wearing corresponding clothes. The clothing images were taken from the front with the clothing in a flat state and the background was pure white. The person body images were taken from the front upper body of the model, and the background was gray or light gray. 14,221 pairs of images are used as the train set, and 2,032 pairs of images are used as the test set.

**MPV** dataset was released by Dong et al. [134] in 2019, which contains 35,687 model images and 13,524 clothing images. The clothing images are the front images of the clothing in the flat state, and the model images are light gray background images. Each model in MPV corresponds to multiple images of different poses, and the image resolution is  $256 \times 192$ . Dong et al. extracted 62,780 triplets of the same person wearing the same clothes but with different poses, further dividing 52,236 triplets as the training set, and shuffling 10,544 triplets as the test set.

**Deep Fashion** [135] is a large-scale dataset released by the Chinese University of Hong Kong. It contains 800,000 images, including different angles, scenes, buyer shows, seller shows, etc. There are four subsets in total, namely: Category and Attribute Prediction Benchmark, In-Shop

Clothes Retrieval Benchmark, Consumer-to-shop Clothes Retrieval Benchmark, and Fashion Landmark Detection Benchmark. The In-Shop Clothes Retrieval Benchmark is often used for virtual try-on tasks, which contains product IDs, images of the same model in different poses, with a resolution of  $1101 \times 750$ . There are a total of 7,982 products corresponding to 52,712 images. Each image is annotated with a bounding box, clothing type, and pose type. Most of the clothes in this dataset are put on bodies with rare separate clothing images.

**VITON-HD** dataset was released by Choi et al. [39] in 2021, which comes from the same source of VITON, but its resolution is kept to  $1024 \times 768$ . As shown in Fig. 6, it additionally contains parsing information such as segmentation, dense pose and pose keypoints. VITON-HD is divided into 11,647 image pairs for training and 2,032 image pairs for testing.

**E-Shop Fashion(ESF)** dataset was proposed by Feng et al. [49] in 2022, which contains 180,000 clothed model photos with adjusted resolution of  $512 \times 512$ . Each image contains a front-standing pose model, and the model image is centrally aligned and filled to the region between the chin and thighs. Furthermore, the dataset is split into a training set containing 170,000 samples and a test set containing 10,000 samples.

**Dress Code** dataset was proposed by Morelli et al. in 2022 [80], which is more than three times larger than the publicly available virtual try-on datasets, with high-resolution paired images ( $1024 \times 768$ ). Different from VITON, which only contains upper-body female image pairs, Dress Code contains upper-body, lower-body, and full-body clothing for both female and male, as well as corresponding model try-on images. The images are divided into three categories: upper-body clothing (consisting of tops, T-shirts, shirts, sweatshirts and sweaters), lower-body clothing (consisting of skirts, pants, shorts, and leggings), and dresses. In total, the dataset consists of 53,795 image pairs: 15,366 pairs for upper-body clothing, 8,951 pairs for lower-body clothing, and 29,478 pairs for dresses. It is divided into a training set containing 48,392 pairs and a test set containing 5,400 pairs (1,800 pairs for upper body, lower body, and full body, respectively). The images are pre-processed and cut at the nose to ensure the privacy of the model. Dress Code also provides pose keypoints, dense pose, and segmentation mask for clothed model images.





Fig. 6. Examples in the dataset. VITON [21] contains pairs of female photo and corresponding in-shop clothing image. MPV [134] consists of triplets of female photos in different poses with the same clothing and the corresponding clothing image. It also parses pose keypoints. Deep Fashion (In-Shop Clothes Retrieval Benchmark) [135] contains images of the same model in different poses. VITON-HD [39] is a high-resolution dataset accompanied with parsed segmentation, dense pose and pose keypoints. ESF [49] consists of clothed model photos for both male and female. Dress Code [80] involves more clothing types and provides dressed model photo, clothing image, pose keypoints, segmentation and dense pose.

In summary, although VITON is the most popular dataset, its limitations include a single type of clothing and a small amount of data. As a ground breaking work for image generation based virtual try-on, it could be used as the most basic benchmark with most works for comparison. However, it restricts the generalization performance. The most recently published Dress Code is a comprehensive dataset with the most diverse types of in-shop clothing images and the widest variety of models for trying on clothes, which should be a good choice for training virtual try-on models at present.

### 3.2 Evaluation Criteria

In this survey, methods are evaluated with previously used criteria such as SSIM (Structural Similarity Index Metric), IS (Inception Score), LPIPS (Learned Perceptual Image Patch Similarity) and FID (Frechet Inception Distance), and a new semantic score. These criteria cover the evaluation in aspects of individual or set comparison, structural or semantic similarity.

**SSIM:** Structural Similarity Index Metric [136] is a traditional image similarity evaluation standard that is originally used for evaluating the performance of image compression algorithms. SSIM index is influenced by the theory of human visual system (HSV) and is calculated from the three aspects of image brightness, contrast and structure. The inputs to compute SSIM are two individual images, i.e., the ground truth image and the generated image. SSIM value ranges within [0,1], where the larger value indicates the smaller difference between the compared two images and the better realism of the generated image. This criterion is

sensitive to pixel shift, so high-level semantic feature is also considered for the evaluation.

**IS:** Inception Score [137] is a metric based on Inception network, which is originally used to evaluate generation models in terms of clarity and diversity. The calculation of IS only involves generated images, and the prediction probability of generated images is used to describe the performance. Clarity refers to more certain probability of belonging to one class, e.g., the prediction entropy is smaller. Diversity involves a set of generated images, where the predictions are evenly distributed across all classes indicate better diversity. The higher value of IS indicate the better generation performance. However, different from the original generation tasks, the generation target for virtual try-on is a fixed class such as human photos. It is not fair enough for this task, and FID becomes an alternative way which compares the distributions of generated images and ground truth.

**FID:** Frechet Inception Distance [138] measures the statistical similarity between two sets of images by calculating the Frechet distance between the feature vectors of the real images and the generated images. Lower value of FID indicate smaller difference between two sets in feature space and better performance.

**LPIPS:** Like IS and FID, Learned Perceptual Image Patch Similarity [139] also utilizes a pretrained network (e.g., VGG [140] and AlexNet [141]) to capture high-level features. It calculates Euclidean or cosine distance between features output via multiple layers. Lower value of LPIPS indicate closer similarity of two images.

**Semantic Score:** We propose a new semantic score with the help of recent advanced model CLIP [53] which connects



text and image. The Euclidean distance between CLIP features of generated image and ground truth is calculated, so lower value indicate closer similarity in semantic information.

It is worth noting that we for the first time separately evaluate the clothing warping performance and generation ability for non-try-on area with a human parser [142]. It further shows which module contributes more to existing methods.

## 4 EXPERIMENTAL RESULTS AND ANALYSIS

Due to the lack of unified evaluation and comprehensive analysis, we run existing open-source codes in image-based virtual try-on area and evaluate them with the same referees. In this section, experimental results are given as quantitative results, qualitative results and user study. Besides the observations towards these results, suggestions in terms of method design are also analyzed.

### 4.1 Quantitative Results

We consider two testing conditions to quantitatively evaluate current representative approaches, i.e., paired condition and unpaired condition. Ground truth exists for paired condition while for unpaired condition the clothes in clothing image and person image are different. Unpaired condition shows a practical scenario but this situation lacks ground truth. With the human parsing method SCHP [142], partial comparisons are proposed for the first time, which separately evaluate the performance of clothing warping (denoted as “clothing”) and generation of non-try-on area (denoted as “person”). More details can be found in the supplement.

The quantitative results of representative methods in the order of publication year are shown in Fig. 7. As unpaired condition lacks ground truth, it is hard to evaluate the generation quality of full body for SSIM, LPIPS and Semantic Score. From the results, we have the following observations:

- Except the results of “Paired Clothing” in terms of SSIM and IS, the overall performance gets better along the development. The poor SSIM performance of clothing warping can be attributed to the damage of clothing patterns.
- On all criteria, the results under paired condition surpass those under unpaired condition. It is understandable that paired testing is a easier task than unpaired situation, as methods are usually trained with paired data.
- By comparing the results of “Paired Clothing” with “Paired Person”, the former falls behind the latter due to the challenges of clothing warping.
- The comparative performance of representative methods on these criteria are roughly consistent, which to some extent show the consistency of evaluation metrics.
- For high-resolution methods, HR-VTON [31] (grey circle) performs better, which attributes to its dual-path pipeline that simultaneously predict human body and clothing and the deformed clothing is further aligned with the predicted semantic segmentation.

### 4.2 Qualitative Results

The qualitative results are displayed in Fig. 8 by showing several cases of image-based virtual try-on. The 1<sup>st</sup> row shows an easy task where the in-shop clothing has the same type as the source image and only contains plain color. Previous methods perform comparatively and the results are satisfying. When changing a piece of clothes with sleeves to a non-sleeve type (e.g., the 2<sup>nd</sup> and 3<sup>rd</sup> row), the sleeves are usually completely removed. However, as shown in the 4<sup>th</sup> row, it is difficult to perfectly fit the sleeves to the person arms. When focusing on the person neck of try-on images, the clothing style is affected by the performance of human parser. The preservation of clothing texture such as special patterns (e.g., the 3<sup>rd</sup> and 5<sup>th</sup> row) and stripes (e.g., the 6<sup>th</sup> row) could be further improved. Person shape (e.g., 3<sup>rd</sup> row) has little effects while challenging pose (e.g., the last row) will increase the difficulty of try-on. Challenging cases will be further discussed in Sec. 5.

From qualitative results, Style-Flow-VTON [38] performs best under low resolution. For earlier works such as VITON [21], SP-VTON [25] and CP-VTON [23] models, the focus is on the processing of the try-on part. When trying on simple clothes, the center area of the clothes has a better generation effect, but the clothes and person parts in the non-try-on area are blurred. LM-VTON [24] and CP-VTON+ [22] have improved the above problems to some extent by preserving the image contents in the non-try-on area, but also contain artifacts. Although DCTON [71] adopts a different model framework from the VITON series, its performance is close to that of LM-VTON and CP-VTON+. The quality of the results generated by PFAFN [37], Style-Flow-VTON [38] and SDAFN [74] gets better, where the boundary between the body area and the clothing area is more natural and clear. It mainly attributes to the warping ability of flow. VITON-HD [39] and HR-VITON [31] are two methods designed for high-resolution virtual try-on, and the results of HR-VITON contain more details.

### 4.3 User Study

In order to assess the visual quality of the virtual try-on results in human perspective, we conducted a survey in the form of a questionnaire to gather feedback from people. The questionnaire consisted of 22 evaluations, where for each algorithm two random samples were selected. Participants were asked to choose one of the five options to rate the quality of the try-on results for each sample: A. 5 (*Very realistic*), B. 4 (*With minor flaws*), C. 3 (*Lack of details*), D. 2 (*Contain obvious artifacts*), and E. 1 (*Messy*). We conducted the testing publicly on the internet and received a total of 333 valid responses from participants. As shown in Fig. 9, the length of the colored areas in the figure represents the proportion of the corresponding evaluation score. The results show that the try-on performance of existing image generation methods is far from satisfactory, which could also be observed in Fig. 8 that humans have high demands from the try-on procedure. It remains a challenging task to generate results with natural warping and clear patterns.

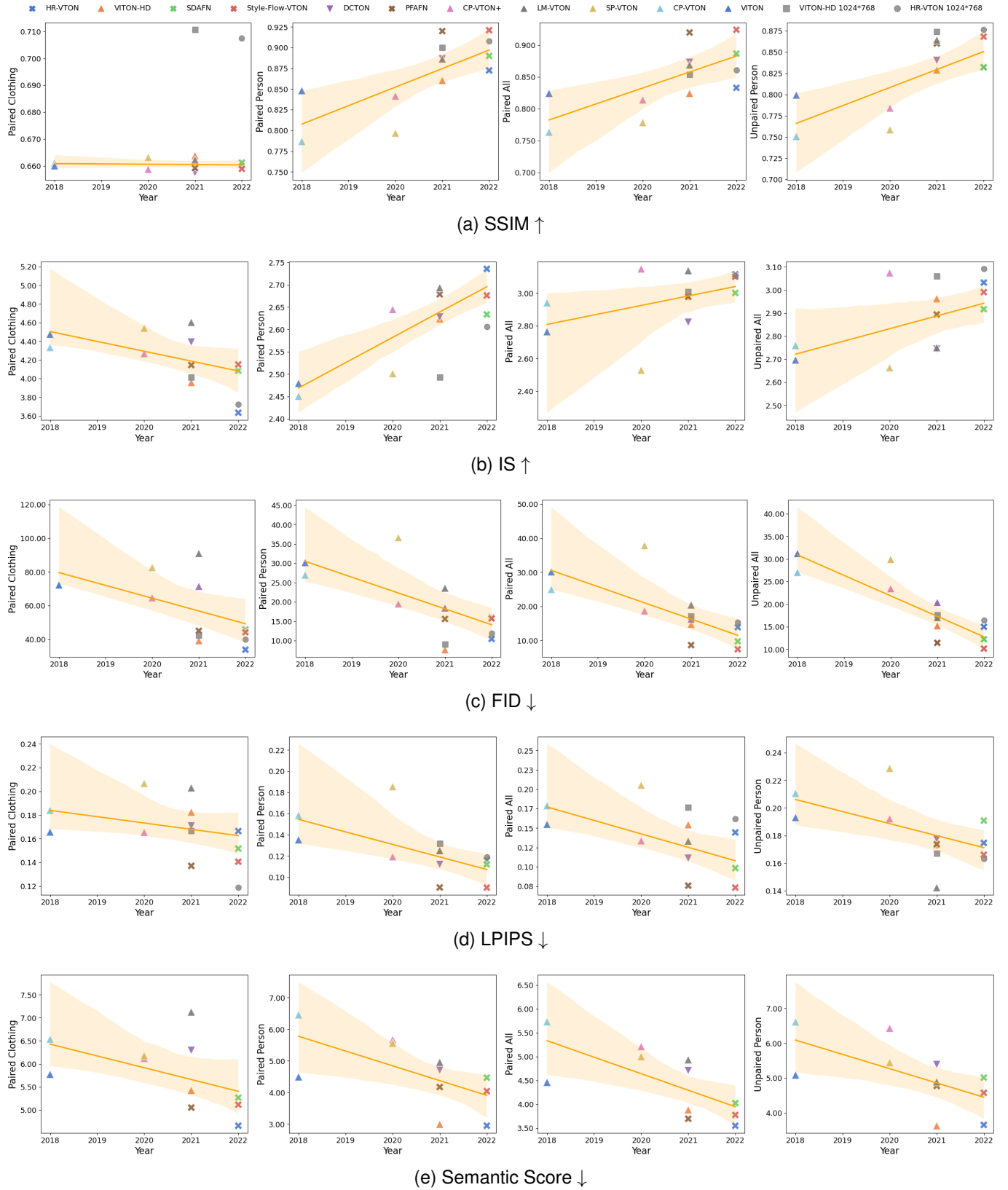


Fig. 7. Quantitative results. The vertical axis indicates the testing condition is paired or unpaired and the evaluation target is clothing, non-try-on area (denoted as “person”) or all together. For method symbol, the cross symbol indicates the clothing warping strategy is flow while the rectangle symbol represents TPS-based method. \*Both HR-VTON and VITON-HD are tested using high-resolution ( $1024 \times 768$ ) datasets. To compare with other low-resolution models, we down-sample the high-resolution results to low resolution ( $256 \times 192$ ). To illustrate the impact of image resolution on evaluation metrics, we denote the scores of high-resolution results with gray points.



Fig. 8. Qualitative results. We show the visual results with variations of person poses, shapes and clothing patterns. Please refer to Sec. 4.2 for detailed analysis.

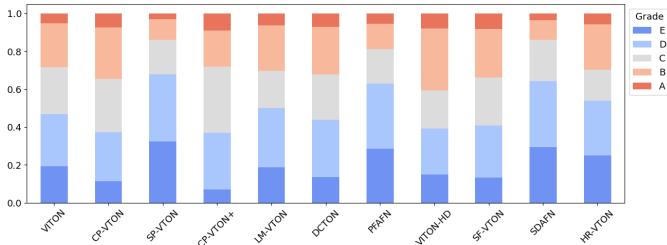


Fig. 9. The user study results on the qualitative results. Participants evaluate the randomly selected try-on images. The length of the colored areas represents the proportion of the corresponding evaluation level where the satisfactory decreases from A to E.

#### 4.4 Discussion on Method Design

By analyzing the experimental results of existing methods, we have the following observations:

- **Pipeline perspective.** The structures of existing pipelines are classified as shown in Fig. 2, and the specific pipeline adopted by each approach is illustrated in Table 1. It could be found that there is no obvious pipeline preference in the development of image-based virtual try-on methods. From both

the quantitative and the qualitative results, the dual-path pipeline (i.e., type VII) achieves superior performance where the dual paths facilitate each other to optimize the generation performance.

- **Clothing warping perspective.** Existing warping approaches adopted by representative methods are shown in Table 1. As illustrated in Sec. 2.5, spatial transformation network (STN) usually cooperates well with thin plate spline (TPS) transformation, and TPS plays a dominating role in the development of clothing warping methods. The performance of clothing warping approaches is reflected as the results of “paired clothing” in Fig. 7, where the rectangle symbol represents TPS-based method and the cross mark denotes flow-based method. Comparatively, the warping method of flow estimation shows superior performance with more flexible transformation.
- **Try-on perspective.** The final try-on performance depends on all procedures including try-on indication, cloth warping and try-on. The generation quality gets better with the development of generative model such as StyleGAN [40]–[42] and Diffusion Model [55], [143].





Fig. 10. Performance under challenging poses. 1<sup>st</sup> row: the results in a classic arms-crossed posture. 2<sup>nd</sup> row: a more challenging case in arms occlusion where the color of sleeves is the same as torso. 3<sup>rd</sup> row: putting on a piece of long-sleeved clothes under the arms-crossed posture. 4<sup>th</sup> row: the fine-grained details of bent wrist cannot be well recovered.

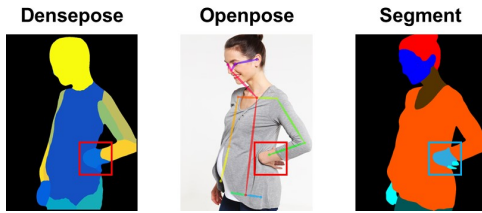


Fig. 11. Coarse pose parsing. Left: human parsing by densepose [58]; Middle: pose keypoints estimated by openpose [60]; Right: semantic parsing via [56]. Current parser lacks fine-grained representation, e.g., the state of fingers at bent wrist.

## 5 UNRESOLVED ISSUES

From previous qualitative results, we can find that try-on results with clear and fine-grained details remain challenging. Apart from this, in this section we further show examples for issues caused by human parsing. Human parsing plays a vital role in image-based virtual try-on, but also causes the main issues due to imperfect parsing ability.

### 5.1 Challenging Poses

Challenging pose usually attributes to the occlusion caused by arms. Take the arm-crossed posture (1<sup>st</sup> row of Fig. 10) for example, three problems should be overcome to perform well: a. correctly judge the position of the arm in front or back of the body and generate the right mask to put on clothes; b. correctly generate the arms and hands in a crossed state; and c. if the try-on is a long-sleeved clothing, correctly handle the relationship between the clothing on the arm and the exposed skin.

For problem a, from Fig. 10 we can find that most methods can tell the front or back position correctly (e.g., the results in 1<sup>st</sup> row) except the ambiguous clothing with plain color (e.g., the results of PFAFN [37] and SDAFN [74] in the 2<sup>nd</sup> row). For problem b, the crossed arms



Fig. 12. The generation of body with challenging poses is alleviated with the help of large-scale models. The try-on results are generated using a slightly modified PBE [55] model as the baseline for validating the virtual try on task based on large models.

are not well solved. HR-VTON [31] and VITON-HD [39] mitigate this problem by optimizing the misaligned parts of the human body and clothing within the generator. The results in the 3<sup>rd</sup> row reflect the model's ability of handling problem c, where the character aims to wear a piece of long-sleeved clothes. Most methods fail to correctly put on sleeves due to the limitation of clothing warping and try-on module. In addition, the arms-crossed pose contains the crossing of the fingers and the arm, which requires high granularity generation ability of the model. Take the 4<sup>th</sup> row for example, current representation such as Openpose [60], Densepose [58] and semantic segmentation map [56], [142] cannot label the fine-grained pose at the wrist (Fig. 11), which fundamentally leads to the poor generation quality.

With the advent of large-scale image generation models [50], [55], [144], the issue of blurred body has been significantly improved. Fig. 12 shows the results that we utilize PBE [55] to inpaint the target clothes to human body. The postures are correctly restored. Thanks to the powerful zero-shot generation capabilities of large-scale models, simple



Fig. 13. Changed clothing styles. The styles of target clothes cannot be preserved due to introducing original clothing information in person representation or clothing bias in the training dataset.

posture features are sufficient to guide the model to generate the correct body. However, it will be pointed out in Sec. 6 that current large-scale models are not fully controllable in terms of the generated contents.

## 5.2 Limited Human Parsing

Besides the pose estimation, image-based virtual try-on methods also rely on some other pre-processing results (as aforementioned in Sec. 2.3). Fig. 14 shows some results generated by HR-VITON and VITON-HD using noisy semantic information, where the wrong parser area has artifacts. It could be found in Fig. 4 that  $\mathcal{P}_{6,7,10,11}$  involve information of original clothes expected to take off. For methods which adopt such representation (e.g., VITON [21], CP-VTON [23] and LM-VTON [24]), the try-on results are affected by the style of original clothes. Take an example for these methods, the collar style of target clothes changes to that of the original clothes as shown in Fig. 13. Unlike these methods, approaches like Style-Flow-VTON [38], VITON-HD [39], and HR-VTON [31], which utilize  $\mathcal{P}_{3,12}$  to address the issue of neckline boundary residuals by redrawing the neckline area, particularly shown in the 3<sup>rd</sup> and 4<sup>th</sup> rows of Fig. 13.

Clothing style is an important aspect to show the performance of virtual try-on, but the current models has poor performance on unconventional styles. From top to bottom in Fig. 13 are short T-shirts, loose-try-on tops, long T-shirts and light tops. Compared with the correct wearing state of the corresponding clothing in the rightmost column of each row, the try-on results generated by the model have obvious biases, and the model tends to make the clothing fit perfectly on the upper body of the person body, presenting a slimming effect. This is unfair for clothing with loose styles or special designs in length, such as the results in the first and third rows, where the short T-shirts are forcibly stretched to the normal length of T-shirts, and the long T-shirts are forcibly reduced/truncated to the normal length of T-shirts. Essentially, the model does not really understand the clothing to be tried on, and it only deforms the



Fig. 14. Artifacts caused by noisy semantic parsing.

clothing image and fills it in the original clothing area for replacement. The main reason attributes to that the model is trained with paired data where target clothes and the clothes on person are actually the same one, and in reality it is difficult to collect unpaired data. Clothing-agnostic person representation still deserve exploration.

## 5.3 Limited Clothing Parsing

Some wrong clothing masks are shown in Fig. 15. Since Style-Flow-VTON rely on the clothing mask [145] to extract “pure clothing image” without background, it heavily relies on the performance of clothing parsing. For clothing with complex textures or similar color as the background, parsed mask usually contains artifacts, which loses important clothing information for final try-on image.

It is worth mention that for large-scale image generation models, e.g., our implemented PBE for virtual try-on, only the character image and clothing image are needed as conditions, and a mask is used to guide the area to be tried on. Due to the strong feature parsing ability and scalability of large image generation models, the dependency on parsing will be also alleviated.





Fig. 15. Failure cases caused by limited clothing parsing. If the target clothes are masked, it is difficult to restore realistic try-on effects.

## 6 FUTURE WORK

Current visual results show that there is still significant room for improvement in image-based virtual try-on methods. On one hand, person representation does not totally get rid of the original clothes, which will affect the clothing style of target clothes. On the other hand, clothing warping approaches are not flexible enough, especially for challenging poses. The emergence of large-scale models alleviates this issue to some extent, but controllable generation becomes a new challenge. In this section, we first continue to show some potential improvements along current research directions in aspects of person representation, clothing deformation, controllable generation, datasets, loss functions and evaluation metrics. Once the quality of generation becomes satisfactory, additional ideas such as size-aware try-on, fashion customization, and scenario-specific generation and so on can also be taken into account.

**Clothing-agnostic person representation.** As the training data is paired where the person already wears target clothes, it will harm the generalization ability if person representation contains clothes information. Current representations  $\mathcal{P}_{3,6,7,10,11}$  in Fig. 4 contains clues from the original clothes such as clothing contour, which will affect the clothing style of target clothes. Totally deleting the body area (i.e.,  $\mathcal{P}_{4,12}$  will get rid of original clothes but lose person characteristics such as skin color. Constructing triplets where a person wears different clothes could be a solution, but current methods [36]–[38] still rely on parser-based methods to construct the triplet, which inherits the limitation of human parser. Future direction could try to construct training triplets with parser-free approaches such as recent large-scale models, or totally delete original clothes but keep a sampler at exposed skin.

**Natural clothing deformation.** Transformation under intrinsic rules such as STN and TPS is limited for flexible deformation. For example, they cannot put sleeves before the torso. Flow estimation learns pixel offset which improves flexibility but cannot generate new pixels that are not displayed in target clothing image but are shown under current posture. Implicit transformation shows potentials



Fig. 16. Generated try-On images by finetuning the stable diffusion model with ControlNet [54]. The generated results are realistic but the clothing patterns are not well preserved.

in clothing deformation and deserves further exploration, especially driven by a 3D deformation model. Additionally, existing methods distort target clothing image into the try-on area and ignore the original style. For example, a cropped top is stretched or a long coat is shrunk to normal length. Fine-grained clothing landmarks could be helpful for this situation.

**Controllable generation with large-scale model.** Large-scale image generation models show powerful generalization and high quality, which is appealing for virtual try-on tasks. However, current models only meet semantic-level control such as satisfying the description from text. More precise and strict control has not been solved such as preserving the original patterns (e.g., Fig 16). To enhance the adaptability of large models for virtual try on tasks, we utilize ControlNet [54] to fine-tune the pre-trained large model [55] with target clothing image as condition. As shown in Fig. 16, the results are natural and realistic but the original patterns are not preserved. In the future, training a specific large-scale model for virtual try-on and preserve original clothing patterns deserve investigation.

**Multi-modal foundation models.** Besides training a specific large-scale model, how to make existing powerful models, e.g., multi-modal foundation models, facilitate virtual try-on task deserves exploration. By incorporating additional modalities, such as textual descriptions or style guidance, multi-modal foundation models can to some extent improve the controllability and customization of the generated virtual try-on images. Furthermore, multi-modal models can leverage the synergistic information from different modalities to enhance the quality of generated images and provide a more immersive and interactive virtual try-on experience.

**Diverse datasets.** Constructing large-scale and diverse virtual try-on datasets forms the foundation of research in this domain. Future datasets should encompass various



types and styles of clothing, as well as diverse human body shapes, poses, and skin tones. Particularly, associated descriptions such as clothing style, size and fabric property are always contained in the website but ignored by existing methods. With the development of cross-modality models, cooperation with these descriptions in image generation might bring benefits.

**Flexible loss functions.** Current training datasets only contain paired samples where the person in image already wears target clothes, so existing loss functions are designed to constrain the full image. However, existing methods cannot generalize well under unpaired evaluation. It is expected to explore flexible loss functions to support unpaired training, which respectively constrains try-on area with target clothing image and non-try-on area from person image.

**Specialized evaluation metrics.** Existing evaluation metrics are not specialized for virtual try-on tasks, and do not reach a consensus with user study. In this paper, a new criteria is proposed with advanced pre-trained model and specifically evaluate the semantic information for try-on and non-try-on areas. Future attention could be paid to assessing the clarity and realism of clothing patterns and the preservation of person characteristics.

**Size-aware try-on.** Existing methods distort target clothing image into the inpainting area with bias towards original clothes. On one hand, the size design of target clothes, e.g., close-fitting or oversized, is ignored. On the other hand, the size of body shapes has not been taken into account. In the future, relative relationship between target clothes and person could be given with several keypoints. How to utilize such information to facilitate the generation process deserves researching.

**Tailorable Try-on.** If size-aware function has been realized, we can further add tailor option by controlling clothing landmarks. For example, we can shorten the length of clothes by moving related landmarks. Further mapping language to landmark movements will make this application more practical.

**Fashion customization.** With the development of large generation models, future try-on tasks can be extended to fashion customization such as changing clothing color, pattern and style. Adding extra patterns can also be easily implemented by putting on specific images.

**Automation and acceleration.** Current methods rely on a series of pre-processing steps, which affects the automation and inference time. More parser-free models can be explored in the future. Additionally, with the diffusion model as the dominant generative framework, addressing its time-consuming sampling process deserves attentions.

**Scenario-specific try-on.** Real-world try-on is limited to dressing rooms, while try-on effects differ in different scenarios such as indoor or outdoor, different seasons and different occasions. Virtual try-on has advantages in synthesizing the background, which provides imaginary space for users to consider the suitability of target clothes. Furthermore, generating videos to showcase the effects in different scenarios would be more engaging.

## REFERENCES

- [1] K. Li, J. Zhang, and D. A. Forsyth, "Povnet: Image-based virtual try-on through accurate warping and residual," *IEEE TPAMI*, vol. 45, no. 10, pp. 12222–12235, 2023.
- [2] F. Cordier, W. Lee, H. Seo, and N. Magnenat-Thalmann, "From 2d photos of yourself to virtual try-on dress on the web," in *BCS HCI/IHM*, 2001, pp. 31–46.
- [3] M. Tang, H. Wang, L. Tang, R. Tong, and D. Manocha, "CAMA: contact-aware matrix assembly with unified collision handling for gpu-based cloth simulation," *Comput. Graph. Forum*, vol. 35, no. 2, pp. 511–521, 2016.
- [4] M. Tang, T. Wang, Z. Liu, R. Tong, and D. Manocha, "I-cloth: incremental collision handling for gpu-based interactive cloth simulation," *ACM Trans. Graph.*, vol. 37, no. 6, p. 204, 2018.
- [5] M. Tang, Z. Liu, R. Tong, and D. Manocha, "PSCC: parallel self-collision culling with spatial hashing on gpus," *Proc. ACM Comput. Graph. Interact. Tech.*, vol. 1, no. 1, pp. 18:1–18:18, 2018.
- [6] C. Cao, Y. Weng, S. Lin, and K. Zhou, "3d shape regression for real-time facial animation," *ACM Trans. Graph.*, vol. 32, no. 4, pp. 41:1–41:10, 2013.
- [7] C. Cao, H. Wu, Y. Weng, T. Shao, and K. Zhou, "Real-time facial animation with image-based dynamic avatars," *ACM Trans. Graph.*, vol. 35, no. 4, pp. 126:1–126:12, 2016.
- [8] C. Cao, D. Bradley, K. Zhou, and T. Beeler, "Real-time high-fidelity facial performance capture," *ACM Trans. Graph.*, vol. 34, no. 4, pp. 46:1–46:9, 2015.
- [9] X. Zhu, X. Liu, Z. Lei, and S. Z. Li, "Face alignment in full pose range: A 3d total solution," *IEEE TPAMI*, vol. 41, no. 1, pp. 78–92, 2019.
- [10] X. Zhu, Z. Lei, J. Yan, D. Yi, and S. Z. Li, "High-fidelity pose and expression normalization for face recognition in the wild," in *CVPR*, 2015, pp. 787–796.
- [11] H. Joo, T. Simon, and Y. Sheikh, "Total capture: A 3d deformation model for tracking faces, hands, and bodies," in *CVPR*, 2018, pp. 8320–8329.
- [12] O. Ronneberger, "Invited talk: U-net convolutional networks for biomedical image segmentation," in *Proceedings des Workshops vom 12. bis 14. März 2017 in Heidelberg*, 2017, p. 3.
- [13] C. Cao, Y. Weng, S. Zhou, Y. Tong, and K. Zhou, "Facewarehouse: A 3d facial expression database for visual computing," *IEEE Trans. Vis. Comput. Graph.*, vol. 20, no. 3, pp. 413–425, 2014.
- [14] D. Song, R. Tong, J. Chang, X. Yang, M. Tang, and J. Zhang, "3d body shapes estimation from dressed-human silhouettes," *Comput. Graph. Forum*, vol. 35, no. 7, pp. 147–156, 2016.
- [15] D. Song, R. Tong, J. Du, Y. Zhang, and Y. Jin, "Data-driven 3-d human body customization with a mobile device," *IEEE Access*, vol. 6, pp. 27 939–27 948, 2018.
- [16] H. Wang, J. F. O'Brien, and R. Ramamoorthi, "Data-driven elastic models for cloth: modeling and measurement," *ACM Trans. Graph.*, vol. 30, no. 4, p. 71, 2011.
- [17] X. He, H. Wang, and E. Wu, "Projective peridynamics for modeling versatile elastoplastic materials," *IEEE Trans. Vis. Comput. Graph.*, vol. 24, no. 9, pp. 2589–2599, 2018.
- [18] Z. Chen, R. Feng, and H. Wang, "Modeling friction and air effects between cloth and deformable bodies," *ACM Trans. Graph.*, vol. 32, no. 4, pp. 88:1–88:8, 2013.
- [19] N. Jetchev and U. Bergmann, "The conditional analogy gan: Swapping fashion articles on people images," in *ICCVW*, 2017, pp. 2287–2292.
- [20] J.-Y. Zhu, T. Park, P. Isola, and A. A. Efros, "Unpaired image-to-image translation using cycle-consistent adversarial networks," in *ICCV*, 2017, pp. 2223–2232.
- [21] X. Han, Z. Wu, Z. Wu, R. Yu, and L. S. Davis, "Viton: An image-based virtual try-on network," in *CVPR*, 2018, pp. 7543–7552.
- [22] M. R. Minar, T. T. Tuan, H. Ahn, P. Rosin, and Y.-K. Lai, "Cp-vton+: Clothing shape and texture preserving image-based virtual try-on," in *CVPRW*, 2020, pp. 10–14.
- [23] B. Wang, H. Zheng, X. Liang, Y. Chen, L. Lin, and M. Yang, "Toward characteristic-preserving image-based virtual try-on network," in *ECCV*, 2018, pp. 589–604.
- [24] G. Liu, D. Song, R. Tong, and M. Tang, "Toward realistic virtual try-on through landmark guided shape matching," in *AAAI*, vol. 35, no. 3, 2021, pp. 2118–2126.
- [25] D. Song, T. Li, Z. Mao, and A.-A. Liu, "Sp-viton: shape-preserving image-based virtual try-on network," *Multimedia Tools and Applications*, vol. 79, pp. 33 757–33 769, 2020.

- [26] H. Yang, R. Zhang, X. Guo, W. Liu, W. Zuo, and P. Luo, "Towards photo-realistic virtual try-on by adaptively generating-preserving image content," in *CVPR*, 2020, pp. 7850–7859.
- [27] K. Ayush, S. Jandial, A. Chopra, M. Hemani, and B. Krishnamurthy, "Robust cloth warping via multi-scale patch adversarial loss for virtual try-on framework," in *ICCVW*, 2019, pp. 1279–1281.
- [28] K. Ayush, S. Jandial, A. Chopra, and B. Krishnamurthy, "Powering virtual try-on via auxiliary human segmentation learning," in *ICCVW*, 2019, pp. 3193–3196.
- [29] H. J. Lee, R. Lee, M. Kang, M. Cho, and G. Park, "LA-VITON: A network for looking-attractive virtual try-on," in *ICCVW*. IEEE, 2019, pp. 3129–3132.
- [30] R. Yu, X. Wang, and X. Xie, "Vtnfp: An image-based virtual try-on network with body and clothing feature preservation," in *ICCV*, 2019, pp. 10511–10520.
- [31] S. Lee, G. Gu, S. Park, S. Choi, and J. Choo, "High-resolution virtual try-on with misalignment and occlusion-handled conditions," in *ECCV*, 2022, pp. 204–219.
- [32] S. Kubo, Y. Iwasawa, M. Suzuki, and Y. Matsuo, "UVTON: UV mapping to consider the 3d structure of a human in image-based virtual try-on network," in *ICCVW*, 2019, pp. 3105–3108.
- [33] A. Neuberger, E. Borenstein, B. Hilleli, E. Oks, and S. Alpert, "Image based virtual try-on network from unpaired data," in *CVPR*, 2020, pp. 5184–5193.
- [34] K. Li, M. J. Chong, J. Zhang, and J. Liu, "Toward accurate and realistic outfits visualization with attention to details," in *CVPR*, 2021, pp. 15546–15555.
- [35] A. Cui, D. McKee, and S. Lazebnik, "Dressing in order: Recurrent person image generation for pose transfer, virtual try-on and outfit editing," in *ICCV*, 2021, pp. 14638–14647.
- [36] T. Issenhuth, J. Mary, and C. Calauzenes, "Do not mask what you do not need to mask: a parser-free virtual try-on," in *ECCV*, 2020, pp. 619–635.
- [37] Y. Ge, Y. Song, R. Zhang, C. Ge, W. Liu, and P. Luo, "Parser-free virtual try-on via distilling appearance flows," in *CVPR*, 2021, pp. 8485–8493.
- [38] S. He, Y.-Z. Song, and T. Xiang, "Style-based global appearance flow for virtual try-on," in *CVPR*, 2022, pp. 3470–3479.
- [39] S. Choi, S. Park, M. Lee, and J. Choo, "Viton-hd: High-resolution virtual try-on via misalignment-aware normalization," in *CVPR*, 2021, pp. 14131–14140.
- [40] T. Karras, S. Laine, and T. Aila, "A style-based generator architecture for generative adversarial networks," in *CVPR*, 2019, pp. 4401–4410.
- [41] T. Karras, S. Laine, M. Aittala, J. Hellsten, J. Lehtinen, and T. Aila, "Analyzing and improving the image quality of stylegan," in *CVPR*, 2020, pp. 8107–8116.
- [42] J. Lin, R. Zhang, F. Ganz, S. Han, and J.-Y. Zhu, "Anycost gans for interactive image synthesis and editing," in *CVPR*, 2021, pp. 14986–14996.
- [43] T. Karras, S. Laine, and T. Aila, "A style-based generator architecture for generative adversarial networks," *IEEE TPAMI*, vol. 43, no. 12, pp. 4217–4228, 2021.
- [44] J. Ho, A. Jain, and P. Abbeel, "Denoising diffusion probabilistic models," in *NeurIPS*, 2020.
- [45] A. Q. Nichol and P. Dhariwal, "Improved denoising diffusion probabilistic models," in *ICML*, 2021, pp. 8162–8171.
- [46] J. Song, C. Meng, and S. Ermon, "Denoising diffusion implicit models," in *ICLR*, 2021.
- [47] F. Croitoru, V. Hondru, R. T. Ionescu, and M. Shah, "Diffusion models in vision: A survey," *IEEE TPAMI*, vol. 45, no. 9, pp. 10850–10869, 2023.
- [48] K. M. Lewis, S. Varadharajan, and I. Kemelmacher-Shlizerman, "Tryongan: Body-aware try-on via layered interpolation," *ACM Trans. Graph.*, vol. 40, no. 4, pp. 1–10, 2021.
- [49] R. Feng, C. Ma, C. Shen, X. Gao, Z. Liu, X. Li, K. Ou, D. Zhao, and Z.-J. Zha, "Weakly supervised high-fidelity clothing model generation," in *CVPR*, 2022, pp. 3440–3449.
- [50] L. Zhu, D. Yang, T. Zhu, F. Reda, W. Chan, C. Saharia, M. Norouzi, and I. Kemelmacher-Shlizerman, "Tryondiffusion: A tale of two unets," in *CVPR*, 2023, pp. 4606–4615.
- [51] A. Jong, M. Moh, and T.-S. Moh, "Virtual try-on with generative adversarial networks: A taxonomical survey," in *Advancements in Computer Vision Applications in Intelligent Systems and Multimedia Technologies*, 2020, pp. 76–100.
- [52] H. Ghodhban, M. Neji, I. Razzak, and A. M. Alimi, "You can try without visiting: a comprehensive survey on virtually try-on outfits," *MTAP*, vol. 81, no. 14, pp. 19967–19998, 2022.
- [53] A. Radford, J. W. Kim, C. Hallacy, A. Ramesh, G. Goh, S. Agarwal, G. Sastry, A. Askell, P. Mishkin, J. Clark *et al.*, "Learning transferable visual models from natural language supervision," in *ICML*, 2021, pp. 8748–8763.
- [54] L. Zhang and M. Agrawala, "Adding conditional control to text-to-image diffusion models," *CoRR*, vol. abs/2302.05543, 2023.
- [55] B. Yang, S. Gu, B. Zhang, T. Zhang, X. Chen, X. Sun, D. Chen, and F. Wen, "Paint by example: Exemplar-based image editing with diffusion models," in *CVPR*, 2023, pp. 18381–18391.
- [56] K. Gong, X. Liang, Y. Li, Y. Chen, M. Yang, and L. Lin, "Instance-level human parsing via part grouping network," in *ECCV*, 2018, pp. 770–785.
- [57] R. Zhang, W. Yang, Z. Peng, P. Wei, X. Wang, and L. Lin, "Progressively diffused networks for semantic visual parsing," *Pattern Recognition*, vol. 90, pp. 78–86, 2019.
- [58] R. A. Güler, N. Neverova, and I. Kokkinos, "Densepose: Dense human pose estimation in the wild," in *CVPR*, 2018, pp. 7297–7306.
- [59] L. Ma, X. Jia, Q. Sun, B. Schiele, T. Tuytelaars, and L. V. Gool, "Pose guided person image generation," in *NeurIPS*, 2017, pp. 406–416.
- [60] Z. Cao, T. Simon, S.-E. Wei, and Y. Sheikh, "Realtime multi-person 2d pose estimation using part affinity fields," in *CVPR*, 2017, pp. 7291–7299.
- [61] J. Duchon, "Splines minimizing rotation-invariant semi-norms in sobolev spaces," in *Constructive Theory of Functions of Several Variables*, 1977, pp. 85–100.
- [62] M. Jaderberg, K. Simonyan, A. Zisserman, and K. Kavukcuoglu, "Spatial transformer networks," in *NeurIPS*, 2015, pp. 2017–2025.
- [63] Y. Li, C. Huang, and C. C. Loy, "Dense intrinsic appearance flow for human pose transfer," in *CVPR*, 2019, pp. 3693–3702.
- [64] A. Raj, P. Sangkloy, H. Chang, J. Lu, D. Ceylan, and J. Hays, "Swapnet: Garment transfer in single view images," in *ECCV*, 2018, pp. 666–682.
- [65] T.-Y. Lin, P. Goyal, R. Girshick, K. He, and P. Dollár, "Focal loss for dense object detection," in *ICCV*, 2017, pp. 2980–2988.
- [66] X. Han, X. Hu, W. Huang, and M. R. Scott, "Clothflow: A flow-based model for clothed person generation," in *ICCV*, 2019, pp. 10471–10480.
- [67] H. Yang, R. Zhang, X. Guo, W. Liu, W. Zuo, and P. Luo, "Towards photo-realistic virtual try-on by adaptively generating-preserving image content," in *CVPR*, 2020, pp. 7850–7859.
- [68] X. Mao, Q. Li, H. Xie, R. Y. Lau, Z. Wang, and S. Paul Smolley, "Least squares generative adversarial networks," in *ICCV*, 2017, pp. 2794–2802.
- [69] T. Miyato, T. Kataoka, M. Koyama, and Y. Yoshida, "Spectral normalization for generative adversarial networks," in *ICLR*, 2018.
- [70] B. Ren, H. Tang, F. Meng, R. Ding, L. Shao, P. H. S. Torr, and N. Sebe, "Cloth interactive transformer for virtual try-on," *CoRR*, vol. abs/2104.05519, 2021.
- [71] C. Ge, Y. Song, Y. Ge, H. Yang, W. Liu, and P. Luo, "Disentangled cycle consistency for highly-realistic virtual try-on," in *CVPR*, 2021, pp. 16928–16937.
- [72] A. Chopra, R. Jain, M. Hemani, and B. Krishnamurthy, "Zflow: Gated appearance flow-based virtual try-on with 3d priors," in *ICCV*, 2021, pp. 5433–5442.
- [73] B. Fele, A. Lampe, P. Peer, and V. Struc, "C-vton: Context-driven image-based virtual try-on network," in *WACV*, 2022, pp. 3144–3153.
- [74] S. Bai, H. Zhou, Z. Li, C. Zhou, and H. Yang, "Single stage virtual try-on via deformable attention flows," in *ECCV*, 2022, pp. 409–425.
- [75] Z. Huang, H. Li, Z. Xie, M. Kampffmeyer, X. Liang *et al.*, "Towards hard-pose virtual try-on via 3d-aware global correspondence learning," in *NeurIPS*, 2022.
- [76] Z. Xie, Z. Huang, X. Dong, F. Zhao, H. Dong, X. Zhang, F. Zhu, and X. Liang, "Gp-vton: Towards general purpose virtual try-on via collaborative local-flow global-parsing learning," in *CVPR*, 2023, pp. 23550–23559.
- [77] K. Yan, T. Gao, H. Zhang, and C. Xie, "Linking garment with person via semantically associated landmarks for virtual try-on," in *CVPR*, 2023, pp. 17194–17204.

- [78] D. Sun, S. Roth, and M. J. Black, "A quantitative analysis of current practices in optical flow estimation and the principles behind them," *Int. J. Comput. Vis.*, vol. 106, no. 2, pp. 115–137, 2014.
- [79] K. Sun, B. Xiao, D. Liu, and J. Wang, "Deep high-resolution representation learning for human pose estimation," in *CVPR*, 2019, pp. 5693–5703.
- [80] D. Morelli, M. Fincato, M. Cornia, F. Landi, F. Cesari, and R. Cucchiara, "Dress code: High-resolution multi-category virtual try-on," in *CVPR*, 2022, pp. 2231–2235.
- [81] O. Ronneberger, P. Fischer, and T. Brox, "U-net: Convolutional networks for biomedical image segmentation," in *MICCAI*, 2015, pp. 234–241.
- [82] A. Vaswani, N. Shazeer, N. Parmar, J. Uszkoreit, L. Jones, A. N. Gomez, L. Kaiser, and I. Polosukhin, "Attention is all you need," in *NeurIPS*, 2017, pp. 5998–6008.
- [83] H. Zunair, Y. Gobeil, S. Mercier, and A. B. Hamza, "Fill in fabrics: Body-aware self-supervised inpainting for image-based virtual try-on," in *BMVC*, 2022, p. 418.
- [84] A. Alisha, C. Amaldev, D. Aysha Dilna, S. Subin, N. Resmi, and G. Sreenu, "Photo-realistic virtual try-on with enhanced warping module," in *ICSAADL*, 2022, pp. 851–862.
- [85] Q. Huang, Z. Zhang, T. Lu, and Y. Zhang, "Cross-category virtual try-on technology research based on pf-afn," in *ICVIP*, 2021, pp. 162–169.
- [86] K. Li, M. J. Chong, J. Liu, and D. A. Forsyth, "Toward accurate and realistic virtual try-on through shape matching and multiple warps," *CoRR*, vol. abs/2003.10817, 2020.
- [87] M. F. Hashmi, B. K. K. Ashish, A. G. Keskar, N. D. Bokde, and Z. W. Geem, "Fashionfit: Analysis of mapping 3d pose and neural body fit for custom virtual try-on," *IEEE Access*, vol. 8, pp. 91 603–91 615, 2020.
- [88] D. Roy, D. Mukherjee, and B. Chanda, "Significance of skeleton-based features in virtual try-on," *CoRR*, vol. abs/2208.08076, 2022.
- [89] B. Ren, H. Tang, F. Meng, R. Ding, L. Shao, P. H. S. Torr, and N. Sebe, "Cloth interactive transformer for virtual try-on," *CoRR*, vol. abs/2104.05519, 2021.
- [90] M. Fincato, F. Landi, M. Cornia, F. Cesari, and R. Cucchiara, "Viton-gt: an image-based virtual try-on model with geometric transformations," in *ICPR*, 2021, pp. 7669–7676.
- [91] V. Mandhana, T. Agrawal, and A. Sardana, "Ndnnet: natural deformation of apparel for better virtual try-on experience," in *SIGAPP*, 2021, pp. 960–966.
- [92] D. L. Pham, N. T. Ngyuen, and S.-T. Chung, "Keypoints-based 2d virtual try-on network system," *Journal of Korea Multimedia Society*, vol. 23, no. 2, pp. 186–203, 2020.
- [93] D. Roy, S. Santra, and B. Chanda, "LGVTON: a landmark guided approach for model to person virtual try-on," *MTAP*, vol. 81, no. 4, pp. 5051–5087, 2022.
- [94] S. Jandial, A. Chopra, K. Ayush, M. Hemani, B. Krishnamurthy, and A. Halwai, "SieveNet: A unified framework for robust image-based virtual try-on," in *WACV*, 2020, pp. 2182–2190.
- [95] A. H. Raffiee and M. Sollami, "Garmentgan: Photo-realistic adversarial fashion transfer," in *ICPR*, 2021, pp. 3923–3930.
- [96] S. Honda, "Viton-gan: Virtual try-on image generator trained with adversarial loss," in *Eurographics*, 2019, pp. 9–10.
- [97] F. Sun, J. Guo, Z. Su, and C. Gao, "Image-based virtual try-on network with structural coherence," in *ICIP*, 2019, pp. 519–523.
- [98] T. Issenhuth, J. Mary, and C. Calauzènes, "End-to-end learning of geometric deformations of feature maps for virtual try-on," *CoRR*, vol. abs/1906.01347, 2019.
- [99] C. Du, F. Yu, M. Jiang, A. Hua, Y. Zhao, X. Wei, T. Peng, and X. Hu, "High fidelity virtual try-on network via semantic adaptation and distributed componentization," *Computational Visual Media*, vol. 8, no. 4, pp. 649–663, 2022.
- [100] Z. Chong and L. Mo, "St-vton: Self-supervised vision transformer for image-based virtual try-on," *Image and Vision Computing*, vol. 127, p. 104568, 2022.
- [101] S. Park and J. Park, "WG-VITON: wearing-guide virtual try-on for top and bottom clothes," *CoRR*, vol. abs/2205.04759, 2022.
- [102] Y. Chang, T. Peng, F. Yu, R. He, X. Hu, J. Liu, Z. Zhang, and M. Jiang, "Vtnct: an image-based virtual try-on network by combining feature with pixel transformation," *The Visual Computer*, pp. 1–14, 2022.
- [103] J. Xu, Y. Pu, R. Nie, D. Xu, Z. Zhao, and W. Qian, "Virtual try-on network with attribute transformation and local rendering," *IEEE TMM*, vol. 23, pp. 2222–2234, 2021.
- [104] Y. Liu, M. Zhao, Z. Zhang, H. Zhang, and S. Yan, "Arbitrary virtual try-on network: Characteristics preservation and trade-off between body and clothing," *CoRR*, vol. abs/2111.12346, 2021.
- [105] H. Zhou, T. Lan, and G. Venkataramani, "PT-VTON: an image-based virtual try-on network with progressive pose attention transfer," *CoRR*, vol. abs/2111.12167, 2021.
- [106] T. Kang, S. Park, S. Choi, and J. Choo, "Data augmentation using random image cropping for high-resolution virtual try-on (VITON-CROP)," *CoRR*, vol. abs/2111.08270, 2021.
- [107] S. Kumar and N. Sinha, "Probing tryongan," in *CODS-COMAD*, 2022, pp. 300–301.
- [108] S. Pecenakova, N. Karessli, and R. Shirvany, "Fitgan: Fit-and shape-realistic generative adversarial networks for fashion," in *ICPR*, 2022, pp. 3097–3104.
- [109] Z. Xie, Z. Huang, F. Zhao, H. Dong, M. Kampffmeyer, X. Dong, F. Zhu, and X. Liang, "PASTA-GAN++: A versatile framework for high-resolution unpaired virtual try-on," *CoRR*, vol. abs/2207.13475, 2022.
- [110] Z. Xie, Z. Huang, F. Zhao, H. Dong, M. Kampffmeyer, and X. Liang, "Towards scalable unpaired virtual try-on via patch-routed spatially-adaptive GAN," in *NeurIPS*, 2021, pp. 2598–2610.
- [111] K. M. Lewis, S. Varadharajan, and I. Kemelmacher-Shlizerman, "VOGUE: try-on by stylegan interpolation optimization," *CoRR*, vol. abs/2101.02285, 2021.
- [112] C. Lin, Z. Li, S. Zhou, S. Hu, J. Zhang, L. Luo, J. Zhang, L. Huang, and Y. He, "RMGN: A regional mask guided network for parser-free virtual try-on," in *IJCAI*, 2022, pp. 1151–1158.
- [113] T. Wang, X. Gu, and J. Zhu, "A flow-based generative network for photo-realistic virtual try-on," *IEEE Access*, vol. 10, pp. 40 899–40 909, 2022.
- [114] S. Pang, X. Tao, N. N. Xiong, and Y. Dong, "An efficient style virtual try on network for clothing business industry," *arXiv preprint arXiv:2105.13183*, 2021.
- [115] Z. Xie, X. Zhang, F. Zhao, H. Dong, M. C. Kampffmeyer, H. Yan, and X. Liang, "Was-vton: Warping architecture search for virtual try-on network," in *ACM MM*, 2021, pp. 3350–3359.
- [116] X. Gao, Z. Liu, Z. Feng, C. Shen, K. Ou, H. Tang, and M. Song, "Shape controllable virtual try-on for underwear models," in *ACM MM*, 2021, pp. 563–572.
- [117] A. Baldrati, D. Morelli, G. Cartella, M. Cornia, M. Bertini, and R. Cucchiara, "Multimodal garment designer: Human-centric latent diffusion models for fashion image editing," *CoRR*, vol. abs/2304.02051, 2023.
- [118] C.-Y. Chen, Y.-C. Chen, H.-H. Shuai, and W.-H. Cheng, "Size does matter: Size-aware virtual try-on via clothing-oriented transformation try-on network," in *ICCV*, 2023, pp. 7513–7522.
- [119] Z. Li, P. Wei, X. Yin, Z. Ma, and A. C. Kot, "Virtual try-on with pose-garment keypoints guided inpainting," in *ICCV*, 2023, pp. 22 788–22 797.
- [120] M. Pernus, C. Fookes, V. Struc, and S. Dobrisek, "FICE: text-conditioned fashion image editing with guided GAN inversion," *CoRR*, vol. abs/2301.02110, 2023.
- [121] Z. Yang, J. Chen, Y. Shi, H. Li, T. Chen, and L. Lin, "Occlumix: Towards de-occlusion virtual try-on by semantically-guided mixup," *IEEE TMM*, vol. 25, pp. 1477–1488, 2023.
- [122] S. Zhang, X. Han, W. Zhang, X. Lan, H. Yao, and Q. Huang, "Limb-aware virtual try-on network with progressive clothing warping," *IEEE TMM*, 2023.
- [123] A. Lin, N. Zhao, S. Ning, Y. Qiu, B. Wang, and X. Han, "Fashion-tex: Controllable virtual try-on with text and texture," in *ACM SIGGRAPH*, 2023, pp. 56:1–56:9.
- [124] K. Nguyen-Ngoc, T. Phan-Nguyen, K. Le, T. V. Nguyen, M. Tran, and T. Le, "DM-VTON: distilled mobile real-time virtual try-on," *CoRR*, vol. abs/2308.13798, 2023.
- [125] S. Pathak, V. Kaushik, and B. Lall, "Single stage warped cloth learning and semantic-contextual attention feature fusion for virtual tryon," *CoRR*, vol. abs/2310.05024, 2023.
- [126] J. Gou, S. Sun, J. Zhang, J. Si, C. Qian, and L. Zhang, "Taming the power of diffusion models for high-quality virtual try-on with appearance flow," *CoRR*, vol. abs/2308.06101, 2023.
- [127] D. Morelli, A. Baldrati, G. Cartella, M. Cornia, M. Bertini, and R. Cucchiara, "Ladi-vton: Latent diffusion textual-inversion enhanced virtual try-on," *CoRR*, vol. abs/2305.13501, 2023.

- [128] M. S. Seyfioglu, K. Bouyarmane, S. Kumar, A. Tavanaei, and I. B. Tutar, "Dreampaint: Few-shot inpainting of e-commerce items for virtual try-on without 3d modeling," *CoRR*, vol. abs/2305.01257, 2023.
- [129] S. Adhikari, B. Bhusal, P. Ghimire, and A. Shrestha, "VTON-IT: virtual try-on using image translation," *CoRR*, vol. abs/2310.04558, 2023.
- [130] S. Belongie, J. Malik, and J. Puzicha, "Shape matching and object recognition using shape contexts," *IEEE TPAMI*, vol. 24, no. 4, pp. 509–522, 2002.
- [131] Y. Ren, X. Yu, J. Chen, T. H. Li, and G. Li, "Deep image spatial transformation for person image generation," in *CVPR*, 2020, pp. 7690–7699.
- [132] M. Loper, N. Mahmood, J. Romero, G. Pons-Moll, and M. J. Black, "Smpl: a skinned multi-person linear model," *ACM Trans. Graph.*, vol. 34, no. 6, pp. 248:1–248:16, 2015.
- [133] T. Park, M.-Y. Liu, T.-C. Wang, and J.-Y. Zhu, "Semantic image synthesis with spatially-adaptive normalization," in *CVPR*, 2019, pp. 2337–2346.
- [134] H. Dong, X. Liang, X. Shen, B. Wang, H. Lai, J. Zhu, Z. Hu, and J. Yin, "Towards multi-pose guided virtual try-on network," in *ICCV*, 2019, pp. 9026–9035.
- [135] Z. Liu, P. Luo, S. Qiu, X. Wang, and X. Tang, "Deepfashion: Powering robust clothes recognition and retrieval with rich annotations," in *CVPR*, 2016, pp. 1096–1104.
- [136] Z. Wang, A. C. Bovik, H. R. Sheikh, and E. P. Simoncelli, "Image quality assessment: from error visibility to structural similarity," *IEEE TIP*, vol. 13, no. 4, pp. 600–612, 2004.
- [137] T. Salimans, I. J. Goodfellow, W. Zaremba, V. Cheung, A. Radford, and X. Chen, "Improved techniques for training gans," in *NeurIPS*, 2016, pp. 2226–2234.
- [138] M. Heusel, H. Ramsauer, T. Unterthiner, B. Nessler, and S. Hochreiter, "Gans trained by a two time-scale update rule converge to a local nash equilibrium," in *NeurIPS*, 2017, pp. 6626–6637.
- [139] R. Zhang, P. Isola, A. A. Efros, E. Shechtman, and O. Wang, "The unreasonable effectiveness of deep features as a perceptual metric," in *CVPR*, 2018, pp. 586–595.
- [140] K. Simonyan and A. Zisserman, "Very deep convolutional networks for large-scale image recognition," in *ICLR*, 2015.
- [141] A. Krizhevsky, I. Sutskever, and G. E. Hinton, "Imagenet classification with deep convolutional neural networks," in *NeurIPS*, 2012.
- [142] P. Li, Y. Xu, Y. Wei, and Y. Yang, "Self-correction for human parsing," *IEEE TPAMI*, vol. 44, no. 6, pp. 3260–3271, 2022.
- [143] R. Rombach, A. Blattmann, D. Lorenz, P. Esser, and B. Ommer, "High-resolution image synthesis with latent diffusion models," in *CVPR*, 2022, pp. 10 684–10 695.
- [144] X. Chen, L. Huang, Y. Liu, Y. Shen, D. Zhao, and H. Zhao, "Anydoor: Zero-shot object-level image customization," *CoRR*, vol. abs/2307.09481, 2023.
- [145] C. Rother, V. Kolmogorov, and A. Blake, "'grabcut' interactive foreground extraction using iterated graph cuts," *ACM Trans. Graph.*, vol. 23, no. 3, pp. 309–314, 2004.

## APPENDIX A

### IMPLEMENTATION DETAILS

The code link for comparison methods and the implementation of evaluation metrics will be given at <https://github.com/little-misfit/Survey-Of-Virtual-Try-On>.

## APPENDIX B

### EVALUATION CRITERIA

Previous methods are quantitatively evaluated in terms of testing conditions and areas. Fig. 17 shows two testing conditions, i.e., paired and unpaired. Paired situation refers to that we have a pair of clothing image and image of person wearing the same clothes. Such data are abundant on the Internet and usually used for training by masking the person image to obtain clothing agnostic person representation. Unpaired situation is close to practical scenario where the clothing in the person image is different from target clothing, where we do not have the ground truth for try-on image. Due to the lack of ground truth, the evaluation criteria such as SSIM, LPIPS and semantic score that rely on paired data do not have unpaired results.



Fig. 17. Two testing conditions are involved for evaluation. Paired evaluation refers to the condition that the clothing image and person image are paired and the clothing-agnostic image is parsed from the person image. Unpaired evaluation refers to that the clothes in the clothing image and person image are different, so there is no ground truth for the try-on result.

We for the first time separately evaluate the generation quality of different areas, i.e., the warped clothing area, the non-try-on area, and the whole area, which are respectively denoted as “Clothing”, “Person” and “All”. Fig. 18 shows several examples for different evaluation areas.

## APPENDIX C

### QUANTITATIVE RESULTS

Fig. 7 draws the quantitative results in charts to better show the relative performance between methods. The original numerical results are shown in Tab. 3, 4, 5, 6 and 7.



Fig. 18. Three testing conditions (“All”, “Person” and “Clothing”). With the help of a parser [142], we separate the generated image to non-try-on area and clothing area. The deleted areas are replaced with black pixel.

TABLE 3  
SSIM  $\uparrow$

| Model                 | Paired Clothing | Paired Person | Paired All   | Unpaired Person |
|-----------------------|-----------------|---------------|--------------|-----------------|
| VITON [21]            | 0.660           | 0.848         | 0.824        | 0.800           |
| CP-VTON [23]          | 0.661           | 0.787         | 0.763        | 0.751           |
| SP-VTON [25]          | 0.663           | 0.797         | 0.778        | 0.759           |
| CP-VTON+ [22]         | 0.659           | 0.842         | 0.814        | 0.784           |
| LM-VTON [24]          | 0.662           | 0.886         | 0.869        | 0.864           |
| PFAFN [37]            | 0.660           | 0.920         | 0.920        | 0.860           |
| DCTON [71]            | 0.657           | 0.887         | 0.873        | 0.840           |
| VITON-HD [39]         | <b>0.664</b>    | 0.860         | 0.824        | 0.829           |
| Style-Flow-VITON [38] | 0.659           | <b>0.921</b>  | <b>0.924</b> | <b>0.868</b>    |
| SDAFN [74]            | 0.661           | 0.890         | 0.887        | 0.832           |
| HR-VTON [31]          | 0.660           | 0.873         | 0.833        | 0.832           |

TABLE 4  
LPIPS  $\downarrow$

| Model                 | Paired Clothing | Paired Person | Paired All   | Unpaired Person |
|-----------------------|-----------------|---------------|--------------|-----------------|
| VITON [21]            | 0.166           | 0.135         | 0.155        | 0.193           |
| CP-VTON [23]          | 0.184           | 0.158         | 0.179        | 0.211           |
| SP-VTON [25]          | 0.207           | 0.185         | 0.205        | 0.229           |
| CP-VTON+ [22]         | 0.165           | 0.119         | 0.134        | 0.192           |
| LM-VTON [24]          | 0.203           | 0.125         | 0.133        | <b>0.142</b>    |
| PFAFN [37]            | <b>0.137</b>    | 0.090         | 0.076        | 0.174           |
| DCTON [71]            | 0.171           | 0.112         | 0.111        | 0.177           |
| VITON-HD [39]         | 0.183           | 0.125         | 0.154        | 0.173           |
| Style-Flow-VITON [38] | 0.141           | <b>0.090</b>  | <b>0.073</b> | 0.166           |
| SDAFN [74]            | 0.152           | 0.112         | 0.098        | 0.191           |
| HR-VTON [31]          | 0.167           | 0.116         | 0.144        | 0.175           |

TABLE 5  
Semantic Score  $\downarrow$

| Model                 | Paired Clothing | Paired Person | Paired All   | Unpaired Person |
|-----------------------|-----------------|---------------|--------------|-----------------|
| VITON [21]            | 5.773           | 4.496         | 4.461        | 5.086           |
| CP-VTON [23]          | 6.535           | 6.457         | 5.730        | 6.613           |
| SP-VTON [25]          | 6.176           | 5.559         | 5.000        | 5.441           |
| CP-VTON+ [22]         | 6.121           | 5.672         | 5.211        | 6.430           |
| LM-VTON [24]          | 7.125           | 4.957         | 4.934        | 4.891           |
| PFAFN [37]            | 5.051           | 4.176         | 3.695        | 4.773           |
| DCTON [71]            | 6.293           | 4.707         | 4.707        | 5.387           |
| VITON-HD [39]         | 5.426           | 2.998         | 3.883        | <b>3.629</b>    |
| Style-Flow-VITON [38] | 5.113           | 4.043         | 3.775        | 4.574           |
| SDAFN [74]            | 5.266           | 4.469         | 4.023        | 5.012           |
| HR-VTON [31]          | <b>4.656</b>    | <b>2.951</b>  | <b>3.549</b> | 3.652           |

## APPENDIX D

### MORE VISUAL RESULTS

All of the testing results will be given at <https://github.com/little-misfit/Survey-Of-Virtual-Try-On>. In terms of clothing style and texture, we show more visual results in Fig. 19.





Fig. 19. More virtual try-on results. The left-most column shows the changing of clothing style and texture. For simplicity, clothing style refers to short sleeve or long sleeve, and clothing texture contains plain color, pattern, stripe and lace.



TABLE 6  
FID ↓

| Model                 | Paired Clothing | Paired Person | Paired All   | Unpaired Clothing | Unpaired Person | Unpaired All  |
|-----------------------|-----------------|---------------|--------------|-------------------|-----------------|---------------|
| VITON [21]            | 72.289          | 30.192        | 30.144       | 86.379            | 32.155          | 31.236        |
| CP-VTON [23]          | 72.856          | 26.963        | 24.969       | 68.908            | 26.827          | 27.048        |
| SP-VTON [25]          | 82.710          | 36.641        | 37.855       | 76.419            | 32.107          | 29.927        |
| CP-VTON+ [22]         | 64.684          | 19.512        | 18.688       | 75.407            | 21.290          | 23.450        |
| LM-VTON [24]          | 90.996          | 23.588        | 20.417       | 64.762            | 17.800          | 17.051        |
| PFAFN [37]            | 45.065          | 15.607        | 8.608        | 49.649            | 16.701          | 11.431        |
| DCTON [71]            | 71.489          | 18.452        | 16.285       | 79.167            | 19.903          | 20.416        |
| VITON-HD [39]         | 39.241          | <b>7.658</b>  | 14.747       | 39.896            | <b>8.012</b>    | 15.223        |
| Style-Flow-VITON [38] | 44.215          | 15.718        | <b>7.395</b> | 48.256            | 16.419          | <b>10.158</b> |
| SDAFN [74]            | 45.835          | 16.056        | 9.707        | 49.902            | 16.467          | 12.226        |
| HR-VTON [31]          | <b>33.847</b>   | 10.459        | 13.878       | <b>35.070</b>     | 11.058          | 14.984        |

TABLE 7  
IS ↑

| Model                 | Paired Clothing | Paired Person | Paired All   | Unpaired Clothing | Unpaired Person | Unpaired All |
|-----------------------|-----------------|---------------|--------------|-------------------|-----------------|--------------|
| VITON [21]            | 4.475           | 2.479         | 2.764        | 4.281             | 2.374           | 2.697        |
| CP-VTON [23]          | 4.332           | 2.451         | 2.941        | 4.072             | 2.384           | 2.759        |
| SP-VTON [25]          | 4.540           | 2.501         | 2.529        | 4.279             | 2.385           | 2.663        |
| CP-VTON+ [22]         | 4.268           | 2.645         | <b>3.148</b> | 4.122             | 2.565           | <b>3.074</b> |
| LM-VTON [24]          | <b>4.603</b>    | 2.693         | 3.137        | 4.056             | 2.606           | 2.750        |
| PFAFN [37]            | 4.144           | 2.679         | 2.978        | 4.197             | 2.632           | 2.894        |
| DCTON [71]            | 4.390           | 2.628         | 2.822        | <b>4.344</b>      | 2.608           | 2.743        |
| VITON-HD [39]         | 3.958           | 2.624         | 2.979        | 4.141             | 2.589           | 2.962        |
| Style-Flow-VITON [38] | 4.150           | 2.676         | 3.100        | 4.133             | 2.609           | 2.991        |
| SDAFN [74]            | 4.084           | 2.633         | 3.001        | 4.012             | 2.597           | 2.917        |
| HR-VTON [31]          | 3.633           | <b>2.736</b>  | 3.114        | 3.609             | <b>2.650</b>    | 3.032        |

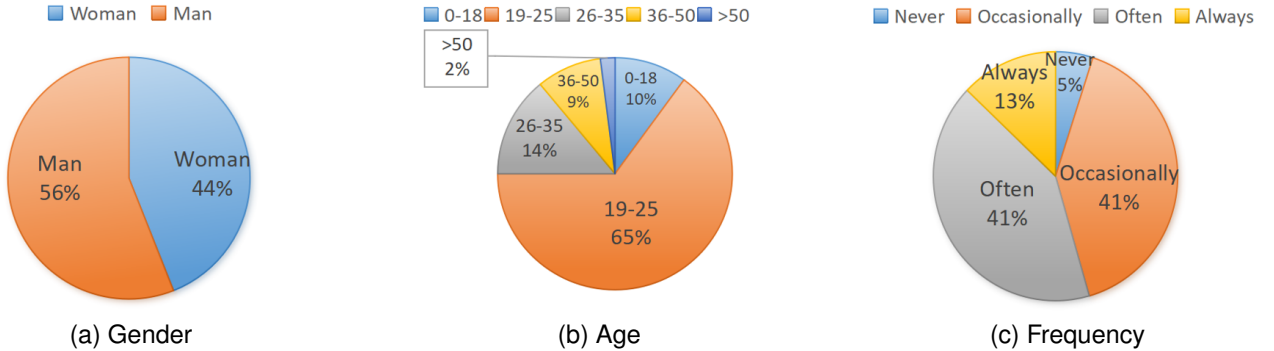


Fig. 20. Demographics of participants in regards of gender, age and frequency of shopping online.

## APPENDIX E

### DEMOGRAPHICS OF PARTICIPANTS

For user study, we released a public link to collect questionnaires. Each questionnaire consists of 22 single-choice questions in regards of the satisfactory towards try-on results, where 2 random examples of 11 methods are selected. The participants voluntarily fill out the questionnaire and receive the bonus upon completing the survey. Demographics of participants are shown in Fig. 20, where the gender ratio is balanced, with a majority of them being young people who engage in online shopping.